horticulturae

MDPI

Article

Lasiodiplodia iraniensis and *Diaporthe* spp. Are Associated with Twig Dieback and Fruit Stem-End Rot of Sweet Orange, *Citrus sinensis*, in Florida

Valeria Piattino [1,2], Dalia Aiello [3], Greta Dardani [1,2], Ilaria Martino [1,2], Mauricio Flores [4], Srđan G. Aćimović [5], Davide Spadaro [1,2], Giancarlo Polizzi [3] and Vladimiro Guarnaccia [1,2,*]

1 Department of Agricultural, Forest and Food Sciences (DISAFA), University of Torino, 10095 Grugliasco, Italy; valeria.piattino@unito.it (V.P.); greta.dardani@unito.it (G.D.); ilaria.martino@unito.it (I.M.); davide.spadaro@unito.it (D.S.)
2 Interdepartmental Centre for the Innovation in the Agro-Environmental Sector, AGROINNOVA, University of Torino, 10095 Grugliasco, Italy
3 Department of Agriculture, Food and Environment (Di3A), University of Catania, 95123 Catania, Italy; dalia.aiello@unict.it (D.A.); gpolizzi@unict.it (G.P.)
4 Keyplex, 400 N. New York Ave Suite 200, Winter Park, FL 32789, USA; labhelechos@yahoo.com.mx
5 Plant Pathology Laboratory, School of Plant and Environmental Sciences, Alson H. Smith Jr. Agricultural Research and Extension Center, Virginia Polytechnic Institute and State University, Winchester, VA 24061, USA; acimovic@vt.edu
* Correspondence: vladimiro.guarnaccia@unito.it

Abstract: Florida ranks among the most important citrus growing regions in the USA. The present study investigates the occurrence, diversity, and pathogenicity of fungal species associated with symptomatic sweet orange (*Citrus sinensis*) cv. Valencia plants and fruit. The survey was conducted on twigs and fruit collected in Southwest Florida during 2022. Based on morphological and molecular characteristics, the identified isolates belonged to the species *Lasiodiplodia iraniensis*, *Diaporthe pseudomangiferae*, and *Diaporthe ueckerae*. The pathogenicity of representative isolates was evaluated on citrus fruit and plants. *Lasiodiplodia iraniensis* was the most virulent on fruit and plants, followed by *Diaporthe pseudomangiferae*. *Diaporthe ueckerae* had the lowest virulence on fruit, and it was not pathogenic to plants. In vitro tests were performed to assess the effect of temperature on mycelial radial growth. The optimum temperature of growth ranged from 26.0 to 28.4 °C for all the evaluated species, and *L. iraniensis* showed the fastest mycelial growth. This study represents the first report of *L. iraniensis* as a causal agent of tree dieback and fruit stem-end rot on *C. sinensis* worldwide. Moreover, *D. pseudomangiferae* and *D. ueckerae* are reported here for the first time in association with citrus diseases worldwide.

Keywords: Botryosphaeriaceae; Diaporthaceae; citrus; pathogenicity; multi-locus phylogeny

Citation: Piattino, V.; Aiello, D.; Dardani, G.; Martino, I.; Flores, M.; Aćimović, S.G.; Spadaro, D.; Polizzi, G.; Guarnaccia, V. *Lasiodiplodia iraniensis* and *Diaporthe* spp. Are Associated with Twig Dieback and Fruit Stem-End Rot of Sweet Orange, *Citrus sinensis*, in Florida. *Horticulturae* **2024**, *10*, 406. https://doi.org/10.3390/horticulturae10040406

Academic Editor: Qiang-Sheng Wu

Received: 29 March 2024
Revised: 11 April 2024
Accepted: 12 April 2024
Published: 17 April 2024

1. Introduction

Citrus is one of the world's most economically important fruit crops, appreciated by consumers for its nutritional value, characterized by a high dose of vitamin C, sugar, organic acids, amino acids, and minerals [1]. Citrus cultivation is distributed in 160 countries of tropical and subtropical regions, spanning six continents on a total area of 12.7 million hectares [2,3]. From 2022 to 2023, 158 million tons of citrus were harvested worldwide [3]. The USA is one of the largest world citrus producers, after China and Brazil, with an economic value of USD 2.91 billion, with California, Florida, Arizona, and Texas representing the main areas [4]. Florida citrus orchards cover about 230,266 hectares, counting more than 74 million citrus trees, which produce 36% of the American citrus. In 2022–2023, 609 tons, including 372 tons of Valencia oranges and 237 tons of non-Valencia oranges, were produced [4].

Several biotic factors affect citrus production and marketing value [5]. Dieback and stem-end rot diseases represent a major threat to citrus cultivation and production in different citrus-producing countries [6–10].

Dieback and twig blight of citrus were reported since the 1900s [11,12] with symptoms such as sunken dark-colored cankers, twig and branch dieback, gummosis, decline, and, in severe cases, plant death [9,13,14]. A wide range of fungal species, which infect wood entering through natural openings or pruning wounds and colonizing vascular tissues, were associated with dieback and trunk diseases [6,15]. Particularly, species belonging to the Botryosphaeriaceae family were reported as causal agents of canker and dieback on citrus, along with *Colletotrichum* spp. and *Diaporthe* spp. [6,13,16–21].

Stem-end rot is one of the most common and economically important decays on all types of citrus fruit in Florida and other hot, humid tropical and subtropical regions of the world [22–24]. The symptoms of stem-end rot appear as small dark brown to black spots, which progress into fruit decay, discoloration, and softening [8,25] and may occur in the field on attached fruit, with subsequent fruit drop. The causal agents of this disease infect fruit at the stem-end before harvest [26]. Several species of Botryosphaeriaceae and *Diaporthe* spp. were identified as causal agents of stem-end rot on citrus [7,27–29].

Botryosphaeriaceae is a cosmopolitan fungal family affecting a broad range of plant hosts [30–32]. Particularly, species of the genera *Diplodia*, *Dothiorella*, *Lasiodiplodia*, *Neofusicoccum*, and *Neoscytalidium* were reported as citrus pathogens [6,9,13,14,16,24,33–37]. In California, several Botryosphaeriaceae species were isolated from necrotic tissues of citrus branch canker and rootstock by Adesemoye et al. [13], including *D. mutila*, *D. seriata*, *D. viticola*, *Doth. iberica*, *L. parva*, *N. australe*, *N. luteum*, *N. mediterraneum*, *N. Parvum*, and *Ne. dimidiatum*.

Diaporthe genus includes pathogens infecting leaves, stems, roots and seeds, endophytes, or saprobes on decaying tissue [38,39]. Pathogenic species cause fruit rot, leaf spot, blight, melanose, canker, dieback, and wilt on a wide range of economically important crops, such as avocado, blueberry, citrus, grapevine, mango, and soybeans [40–46]. Several species of *Diaporthe* were reported in association with citrus diseases [19,47]. In Europe, Guarnaccia et al. [18] reported *Dia. limonicola* and *Dia. melitensis* as causal agents of severe woody cankers on *C. limon* and isolated *Dia. foeniculina* from eight *Citrus* species (Bergamot orange, *C. bergamia*; round kumquat, *C. japonica*; lemon, *C. limon*; pomelo, *C. maxima*; Calamansi *C. mitis*; grapefruit, *C. paradisi*; mandarin orange, *C. reticulata*, and sweet orange, *C. sinensis*). Moreover, Udayanga et al. [47] recovered *Dia. cytosporella* from symptomatic citrus in Spain, Italy, and the USA. *Dia. citri* is considered one of the most important pathogens of citrus that is widespread on several hosts, including *C. limon*, *C. maxima*, *C. paradisi*, *C. reticulata*, and *C. sinensis* [47–52].

During 2022, dieback and stem-end rot symptoms were observed in several citrus orchards in different areas in Florida. Considering the high economic importance of citrus industry in Florida and the serious threat posed by Botryosphaeriaceae and *Diaporthe* species, an extensive survey was conducted with the aim to (1) assess the presence of fungal species associated with the dieback and stem-end rot, (2) provide accurate identification of the species through molecular analysis and phylogenies, (3) assess the morphological characteristics of the species found and temperature effect on their mycelial growth rate, and (4) evaluate pathogenicity on citrus fruit and plants.

2. Materials and Methods

2.1. Field Sampling and Fungal Isolation

Field surveys were performed from April to October 2022 in thirty-five citrus orchards in South-central Florida (Figure 1; Table 1). Twigs and fruit samples were collected from symptomatic trees of *Citrus sinensis* cv. Valencia, aged between 3 and 12 years, and showed dieback and stem-end rot symptoms (Figure 2). The symptomatic samples were surface disinfected with 1.5% sodium hypochlorite for 60 s, washed twice in sterile distilled water (SDW), and dried on sterile absorbent paper. Small pieces (5 × 5 mm) were cut from the

margin of necrotic lesions and placed on potato dextrose agar (PDA, VWR Chemicals, Leuven, Belgium) Petri dishes with 25 mg L^{-1} of streptomycin sulphate (Sigma-Aldrich, St. Louis, MO, USA) (PDA-S). Plates were incubated at 25 ± 1 °C under 12 h photoperiod for 2–4 days, and pure cultures were obtained by transferring mycelial plugs from the margins of the growing colony on new PDA-S plates.

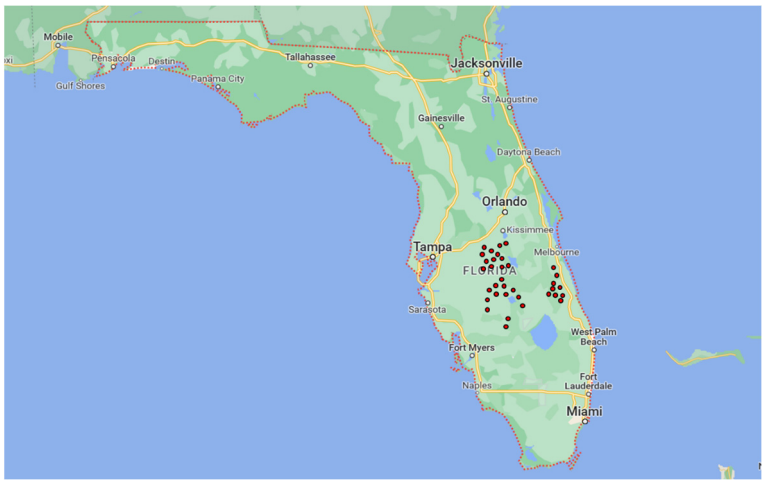

Figure 1. Geographical distribution of the 35 sampled citrus orchards in Florida. Red dots represent sampled areas.

Figure 2. Symptoms caused by *Diaporthe* spp. and *Lasiodiplodia* spp. on *Citrus sinensis* cv. Valencia in Florida. (**a**,**b**) Stem-end rot on ripe fruit; (**c**,**d**) twig and branch dieback.

Table 1. Location and GPS coordinates of the sampled citrus orchards in Florida.

Locality	Orchard	GPS Coordinates
Groves	1	27.5471351 N–81.6733289 W
Sebring	2	27.1606129 N–81.3105547 W
	3	27.1597714 N–81.3176948 W
	4	27.50406 N–81.33028 W
	5	27.50373 N–81.34373 W
	6	27.50437 N–81.22116 W
	7	27.28401 N–81.13406 W
	8	27.28227 N–81.17358 W
DeSoto County	9	27.3130647 N–81.6936935 W
	10	27.2813967 N–81.7091179 W
Polk County	11	27.976646 N–81.48899 W
	12	27.95506 N–81.471910 W
St. Lucie County School District	13	27.4730 N–80.62818 W
	14	27.48017 N–80.62691 W
	15	27.46471 N–80.62985 W
	16	27.49084 N–80.62699 W
	17	27.45678 N–80.49815 W
	18	27.45860 N–80.51303 W
	19	27.45855 N–80.50092 W
Lakeland	20	27.84340 N–81.57374 W
	21	27.88448 N–81.54064 W
	22	27.55239 N–81.34291 W
	23	27.92471 N–81.47095 W
	24	27.92141 N–81.6386 W
	25	27.87577 N–81.55236 W
Lake Wales	26	27.55475 N–81.33492 W
	27	27.55481 N–81.33383 W
	28	27.55232 N–81.34283 W
	29	27.56271 N–81.33534 W
	30	27.553237 N–81.34307 W
Osceola County	31	28.15235 N–81.41578 W
	32	28.09085 N–81.24568 W
Hillcrest Heights	33	27.82674 N–81.53213 W
Indian River County School District	34	27.81489 N–80.62050 W
	35	27.62212 N–80.6298 W

2.2. Molecular Characterization

A total of 0.1 g of mycelium grown on PDA-S at 25 ± 1 °C for 7 days was scraped to extract DNA using E.Z.N.A fungal DNA Mini-Kit (Omega Bio-Tek, Darmstadt, Germany) following the provided instructions. The identification of isolates (Table S1) was achieved by DNA amplification and sequencing of a combined data set of 3 loci: the nuclear ribosomal internal transcribed spacer (ITS) region, the *translation elongation factor 1-α* (*tef1*), and *β-tubulin* genomic regions (*tub2*). Amplification of ITS was performed using the primers ITS1/ITS4 [53], while the primers EF1-728F/EF1-986R [54] were used to amplify the partial *tef1* gene. The *tub2* locus was partially amplified with primers T1/Bt2b [55,56]. The PCR amplification mixtures and thermal conditions adopted for all the considered loci were performed as described by Pavlic et al. [57] and Slippers et al. [31]. For each PCR reaction, 5 µL of PCR product were used to assess amplification by electrophoresis at 100 V on 1% agarose gels (VWR Life Science AMRESCO® biochemicals) stained with GelRed™. PCR amplicons were sequenced by Eurofins Genomics Service (Cologne, Germany). The obtained DNA sequences were analyzed using Geneious v. 11.1.5 (Auckland, New Zealand).

2.3. Phylogenetic Analyses

DNA sequences were compared with NCBI's GenBank nucleotide database through the standard nucleotide Basic Local Alignment Search Tool (BLAST) [58] to determine the closest taxonomic species of the studied isolates. The three genomic regions, which included both the newly obtained sequences and the reference sequences downloaded from GenBank, were aligned using MAFFT v. 7 online server (http://mafft.cbrc.jp/alignment/server/index.html accessed on 1 November 2023) [59] and then manually adjusted in MEGA v. 7 when necessary [60]. Phylogenetic analyses were performed individually for each locus and then as multi-locus analyses of three concatenated loci. The reference sequences were selected based on recent studies on the family Botryosphaeriaceae and the genus *Diaporthe* [6,19,46,61,62] (Table 2). *Dothiorella viticola* (CBS 117009) was selected as outgroup for species belonging to the Botryosphaeriaceae [6]. *Diaporthella corylina* (CBS 121124) was used as outgroup for *Diaporthe* spp. [19]. Multi-locus phylogenetic analyses were performed based on Bayesian Inference (BI) and Maximum Parsimony (MP) criteria. For BI analyses, the best evolutionary model was estimated using MrModeltest v. 2.3 [63] for each partition and included in the analyses. MrBayes v. 3.2.5 [64] was used to generate the best phylogenetic tree based on optimal setting criteria for each locus through Markov Chain Monte Carlo (MCMC) method. The MCMC analyses, which started from a random tree topology, used four chains. Pre-burn and heating parameters were set to 0.25 and 0.2, respectively. The trees were sampled every 1000 generations, and the analyses ended when the average standard deviation of split frequencies was lower than 0.01. Multi-locus analyses based on the MP criterion were performed with Phylogenetic Analyses Using Parsimony (PAUP) v. 4.0b10 [65]. Phylogenetic relationships were established by heuristic searches with 100 random additional sequences. Tree bisection reconnection (TBR) was used with branch swapping option on "best trees" with all characters weighted equally and alignment gaps considered as fifth base. Tree length (TL), consistency index (CI), retention index (RI), and rescaled consistency index (RC) were calculated to estimate parsimony. Bootstrap analyses were based on 1000 replications and the obtained trees were visualized with FigTree version 1.6.6 [66]. Sequences generated in this study were deposited in GenBank (Table 2).

2.4. Morphological Characterization

Based on the results obtained from molecular characterization, five representative isolates of Botryosphaeriaceae (CVG 1930, CVG 1945, CVG 1980, CVG 2155, CVG 2160) and four of *Diaporthe* spp. (CVG 1937, CVG 1938, CVG 2045, CVG 2046) were selected to evaluate their morphology. Agar plugs (6 mm diam) were transferred from actively growing cultures to the center of fresh Petri dishes containing PDA-S. Isolates of *Lasiodiplodia* were placed onto the center of Petri dishes containing 2% water agar supplemented with sterile pine needles (Pine Needles agar or PNA) [67], while isolates of *Diaporthe* were transferred onto malt extract agar (MEA; Oxoid, Fisher Scientific, Pittsburg, PA, USA) to induce sporulation. Plates were incubated at 25 ± 1 °C under a 12 h photoperiod. Colony characteristics of *Lasiodiplodia* and *Diaporthe* were observed after 10 days, and colors were determined according to Rayner [68]. Cultures were examined daily for conidiomata development. Conidia characteristics were observed by mounting fungal structures in SDW. The length and width of 100 conidia were measured for each isolate using an optic microscope (40× magnification). Average length and width, as well as standard deviations were calculated.

Table 2. Collection details and GenBank accession numbers of isolates included in this study.

Species	Isolate Code [1]	Host	Country	GenBank Accession Number [2]		
				ITS	*tef1*	*tub2*
Diaporthe alnea	**CBS 146.46**	Betulaceae	Netherlands	KC343008	KC343734	KC343976
Diaporthe arengae	**CBS 114979**	*Arenga engleri*	Hong Kong	KC343034	KC343760	KC344002
Diaporthe baccae	**CBS 136972**	*Vaccinium corymbosum*	Italy	KJ160565	KJ160597	MF418509
	CBS 142545	*Citrus sinensis* cv. Tarocco	Italy	MF418351	MF418430	MF418519
Diaporthe betulae	**CFCC 50469**	*Betula platyphylla*	China	KT732950	KT733016	KT733020
	CFCC 50470	*Betula platyphylla*	China	KT732951	KT733017	KT733021
Diaporthe biconispora	**ICMP20654**	*Citrus grandis*	China	KJ490597	KJ490476	KJ490418
Diaporthe biguttusis	**CGMCC 3.17081**	*Lithocarpus glabra*	China	KF576282	KF576257	KF576306
Diaporthe celastrina	CBS 139.27	*Celastrus* sp.	USA	KC343047	KC343773	KC344015
Diaporthe citri	CBS 134239	*Citrus sinensis*	USA, Florida	KC357553	KC357522	KC357456
	CBS 135422	*Citrus* sp.	USA	KC843311	KC843071	KC843187
Diaporthe citrichinensis	**CBS 134242**	*Citrus* sp.	China	JQ954648	JQ954666	MF418524
Diaporthe convolvuli	FAU649	*Convolvulus arvensis*	Canada	KJ590721	KJ590765	-
	CBS 124654	*Convolvulus arvensis*	Turkey	KC343054	KC343780	KC344022
Diaporthe ellipicola	**CGMCC 3.17084**	*Lithocarpus glabra*	China	KF576270	KF576245	KF576294
Diaporthe endophytica	**CBS 133811**	*Schinus terebinthifolius*	Brazil	KC343065	KC343791	KC344033
Diaporthe eres	CBS 439.82	*Cotoneaster* sp.	Scotland	KC343090	KC343816	KC344058
Diaporthe foeniculina	CBS 111553	*Foeniculum vulgare*	Spain	KC343101	KC343827	KC344069
	CBS 135430	*Citrus limon*	USA	KC843301	KC843110	KC843215
Diaporthe hongkongensis	**CBS 115448**	*Dichroa febrifuga*	China	KC343119	kc343845	KC344087
Diaporthe inconspicua	**CBS 133813**	*Maytenus ilicifolia*	Brazil	KC343123	KC343849	KC344091
Diaporthe limonicola	**CBS 142549**	*Citrus limon*	Malta, Gozo	MF418422	MF418501	MF418582
	CBS 142550	*Citrus limon*	Malta, Zurrieq	MF418423	MF418502	MF418583

Table 2. *Cont.*

Species	Isolate Code [1]	Host	Country	GenBank Accession Number [2]		
				ITS	*tef1*	*tub2*
Diaporthe logicolla	**ATCC 60325**	*Glycine max*	USA	KJ590728	KJ590767	KJ610883
	CBS 116023	*Glycine max*	USA	KC343198	KC343924	KC344166
Diaporthe melitensis	**CBS 142551**	*Citrus limon*	Malta, Gozo	MF418424	MF418503	MF418584
	CBS 142552	*Citrus limon*	Malta, Gozo	MF418425	MF418504	MF418585
Diaporthe multiguttulata	ICMP20656	*Citrus grandis*	China	KJ490633	KJ490512	KJ490454
Diaporthe neilliae	CBS 144. 27	*Spiraea* sp.	USA	KC343144	KC343870	KC344112
Diaporthe phoenicicola	CBS 161.64	*Areca catechu*	India	KC343032.1	KC343758.1	KC344000.1
Diaporthe pseudomangiferae	**CBS 101339**	*Mangifera indica*	Dominican Republic	KC343181	KC343907	KC344149
	CVG 2045	*Citrus sinensis* cv. Valencia	USA, Florida	PP312931	PP329599	PP329603
	CVG 2046	*Citrus sinensis* cv. Valencia	USA, Florida	PP312932	PP329600	PP329604
Diaporthe pseudophoenicicola	**CBS 462.69**	*Phoenix dactylifera*	Spain	KC343184	KC343910	KC344152
Diaporthe pulla	**CBS 338.89**	*Hedera helix*	Yugoslavia	KC343152	KC343878	KC344120
Diaporthe saccarata	**CBS 116311**	*Protea repens*	South Africa	KC343190	KC343916	KC344158
Diaporthe sojae	**CBS 139282**	*Glycine max*	USA	KJ590719	KJ590762	KJ610875
	CBS 116019	*Caperonia palustris*	USA	KC343175	KC343901	KC344143
Diaporthe uekeri	**CBS 139283**	*Cucumis melo*	USA, Oklahoma	NR 147543	OM370952	OM370953
	FAU656	*Cucumis melo*	USA	KJ590726	KJ590747	KJ610881
	CVG 1937	*Citrus sinensis* cv. Valencia	USA, Florida	PP312929	PP329597	PP329601
	CVG 1938	*Citrus sinensis* cv. Valencia	USA, Florida	PP312930	PP329598	PP329602
Diaporthe unshiuensis	CGMCC 3.17569	*Citrus unshiu*	China	KJ490587	KJ490466	KJ490408
Diaporthella corylina	**CBS 121124**	*Corylus* sp.	China	KC343004	KC343488	KC343972
Dothiorella viticola	CBS 117009	*Citrus sinensis*, twig	Italy	AY905554	AY905559	EU673104
Lasiodiplodia acaciae	**CBS 136434**	*Acacia* sp., leaf spot	Indonesia	MT587421	MT592133	MT592613

Table 2. *Cont.*

Species	Isolate Code [1]	Host	Country	GenBank Accession Number [2]		
				ITS	*tef1*	*tub2*
Lasiodiplodia avicenniae	**CMW 41467**	*Avicennia marina*	South Africa	KP860835	KP860680	KP860758
Lasiodiplodia brasiliensis	**CMM4015**	*Mangifera indica*	Brazil	JX464063	JX464049	-
	CMM4469	*Anacardium occidentale*	Brazil	KT325574.1	KT325580.1	-
Lasiodiplodia bruguierae	**CMW 41470**	*Bruguiera gymnorrhiza*	South Africa	NR_147358	KP860678	KP860756
Lasiodiplodia chiangraiensis	**MFLUCC 21- 0003**	**-**	Thailand	MW760854	MW815630	MW815628
	GZCC 21- 0003	-	Thailand	MW760853	MW815629	MW815627
Lasiodiplodia cinnamomi	CFCC 51997	*Cinnamomum camphora*	China	MG866028	MH236799	MH236797
	CFCC 51998	*Cinnamomum camphora*	China	MG866029	MH236800	MH236798
Lasiodiplodia citricola	**CBS 124707**	*Citrus* sp.	Iran	GU945354	GU945340	KP872405
	CBS 124706	*Citrus* sp.	Iran	GU945353	GU945339	KU887504
Lasiodiplodia endophytica	**MFLUCC 18-1121**	*Magnolia candolii*	China	MK501838	MK584572	MK550606
Lasiodiplodia egyptiacae	**CBS 130992**	*Mangifera indica*	Egypt	JN814397	JN814424	–
Lasiodiplodia euphorbiaceicola	**CMM 3609**	*Jatropha curcas*	Brazil	KF234543	KF226689	KF254926
	CMW 33268	*Adansonia* sp.	Senegal	KU887131	KU887008	KU887430
Lasiodiplodia exigua	**CERC 1961**	*Pistacia vera* cv. Kerman, twigs	USA, Arizona	KP217059	KP217067	KP217075
Lasiodiplodia gravistriata	CMM 4564	*Anacardium humile*	Brazil	KT250949.1	KT250950	–
Lasiodiplodia gilanensis	**IRAN 1523C**	*Citrus* sp., fallen twigs	Iran	GU945351	GU945342	KP872411
	IRAN1501C	*Citrus* sp.	Iran	GU945352	GU945341	KU887510
Lasiodiplodia gonubiensis	**CBS 115812**	*Syzygium cordatum*	South Africa	AY639595	DQ103566	DQ458860
Lasiodiplodia hyalina	CGMCC 3.17975	*Acacia confusa*	China	KX499879	KX499917	KX499992
	CGMCC 3.18383	*woody plant*	China	KY767661	KY751302	KY751299
Lasiodiplodia hormozganensis	**IRAN 1500C**	*Olea* sp.	Iran	GU945355	GU945343	KP872413
	IRAN1498C	*Mangifera indica*	Iran	GU945356	GU945344	KU887514

Table 2. *Cont.*

Species	Isolate Code [1]	Host	Country	GenBank Accession Number [2]		
				ITS	***tef1***	***tub2***
	CBS 124710; IRAN 1520C	*Salvadora persica*, twigs	Iran	GU945346	GU945334	KP872415
	CMW 33252	*Adansonia* sp.	-	KU887065	KU886947	KU887422
	CMW 33333	*Adansonia* sp.	-	KU887085	KU886963	KU887448
	CMW 35881	*Adansonia* sp.	-	KU887092	KU886970	KU887464
	CMW 33311	*Adansonia* sp.	-	KU887084	KU886962	KU887442
	IRAN1502C	*Juglans* sp.	Iran	GU945347	GU945335	KU887517
	CMM 3610	*Jatropha curcas*	Brazil	KF234544	KF226690	KF254927
	CBS 111005; STE-U 1136; CPC 1136	-	-	MT587430	MT592142	MT592624
	CBS 111008; STE-U 1135; CPC 1135	-	-	MT587431	MT592143	MT592625
	CBS 124711; IRAN 1502C	*Juglans* sp., twigs	Iran	GU945347	GU945335	KU887517
Lasiodiplodia iraniensis	*CVG 1905*	*Citrus sinensis* cv. Valencia	USA, Florida	PP309948	PP389256	PP319979
	CVG 1906	*Citrus sinensis* cv. Valencia	USA, Florida	PP309949	PP389257	PP319980
	CVG 1929	*Citrus sinensis* cv. Valencia	USA, Florida	PP309950	PP389258	PP319981
	CVG 1930	*Citrus sinensis* cv. Valencia	USA, Florida	PP309951	PP389259	PP319982
	CVG 1944	*Citrus sinensis* cv. Valencia	USA, Florida	PP309952	PP389260	PP319983
	CVG 1945	*Citrus sinensis* cv. Valencia	USA, Florida	PP309953	PP389261	PP319984
	CVG 1957	*Citrus sinensis* cv. Valencia	USA, Florida	PP309954	PP389262	PP319985
	CVG 1979	*Citrus sinensis* cv. Valencia	USA, Florida	PP309955	PP389263	PP319986
	CVG 1980	*Citrus sinensis* cv. Valencia	USA, Florida	PP309956	PP389264	PP319987
	CVG 1985	*Citrus sinensis* cv. Valencia	USA, Florida	PP309957	PP389265	PP319988
	CVG 1987	*Citrus sinensis* cv. Valencia	USA, Florida	PP309958	PP389266	PP319989
	CVG 1988	*Citrus sinensis* cv. Valencia	USA, Florida	PP309959	PP389267	PP319990
	CVG 1996	*Citrus sinensis* cv. Valencia	USA, Florida	PP309960	PP389268	PP319991

Table 2. *Cont.*

Species	Isolate Code [1]	Host	Country	GenBank Accession Number [2]		
				ITS	*tef1*	*tub2*
Lasiodiplodia iraniensis	*CVG 2000*	*Citrus sinensis* cv. Valencia	USA, Florida	PP309961	PP389269	PP319992
	CVG 2001	*Citrus sinensis* cv. Valencia	USA, Florida	PP309962	PP389270	PP319993
	CVG 2048	*Citrus sinensis* cv. Valencia	USA, Florida	PP309963	PP389271	PP319994
	CVG 2049	*Citrus sinensis* cv. Valencia	USA, Florida	PP309964	PP389272	PP319995
	CVG 2155	*Citrus sinensis* cv. Valencia	USA, Florida	PP309965	PP389273	PP319996
	CVG 2156	*Citrus sinensis* cv. Valencia	USA, Florida	PP309966	PP389274	PP319997
	CVG 2160	*Citrus sinensis* cv. Valencia	USA, Florida	PP309967	PP389275	PP319998
	CVG 2161	*Citrus sinensis* cv. Valencia	USA, Florida	PP309968	PP389276	PP319999
	CVG 2166	*Citrus sinensis* cv. Valencia	USA, Florida	PP309969	PP389277	PP320000
Lasiodiplodia lignicola	CBS 342.78	*Sterculia oblonga*	Germany	KX464140	KX464634	KX464908
	CGMCC 3.18061	Woody branch	China	KX499889	KX499927	KX500002
Lasiodiplodia laeliocattleyae	**CBS 167.28**	*Laeliocattleya*	Italy	KU507487	KU507454	-
	CBS 130992	*Mangifera indica*	Egypt	NR_120002	KU507454	KU887508
Lasiodiplodia macrospora	**CMM 3833**	*Jatropha curcas*	Brazil	KF234557	KF226718	KF254941
Lasiodiplodia magnoliae	**MFLUCC 18-0948**	*Magnolia candolii*, dead leaves	China	MK499387	MK568537	MK521587
Lasiodiplodia mahajangana	**CBS 124925; CMW 27801**	*Terminalia catappa*	Madagascar	FJ900595	FJ900641	FJ900630
Lasiodiplodia mediterranea	**CBS 137783**	*Quercus ilex*, branch canker	Italy	KJ638312	KJ638331	-
Lasiodiplodia microconidia	**CGMCC 3.18485**	*Aquilaria crassna*	Laos	KY783441	KY848614	-
Lasiodiplodia parva	**CBS 456.78**	*Cassava field*	Colombia	EF622083	EF622063	KP872419
Lasiodiplodia plurivora	**STE-U 5803**	*Prunus salicina*	South Africa	EF445362	EF445395	KP872421
	STE-U 4583	*Vitis vinifera*	South Africa	AY343482	EF445396	KU887525
Lasiodiplodia pontae	CMM 1277	*Spondias purpure*	Brazil	KT151794	KT151791	KT151797
Lasiodiplodia pseudotheobromae	**CBS 116459**	*Gmelina arborea*	Costa Rica	EF622077	EF622057	EU673111
	CBS 304.79	*Rosa* cv. Ilona, branches	Netherlands	EF622079	EF622061	MT592630

Table 2. *Cont.*

Species	Isolate Code [1]	Host	Country	GenBank Accession Number [2]		
				ITS	***tef1***	***tub2***
Lasiodiplodia subglobosa	**CMM 3872**	*Jatropha curcas*	Brazil	KF234558	KF226721	KF254942
Lasiodiplodia thailandica	**CPC 22795**	*Mangifera indica*	Thailand	KJ193637	KJ193681	-
Lasiodiplodia theobromae	**CBS 164.96**	Fruit along coral reef coast	Papua New Guinea	AY640255	AY640258	EU673110
Lasiodiplodia tropica	**CGMCC 3.18477**	*Aquilaria crassna*	Laos	KY783454	KY848616	KY848540
Lasiodiplodia viticola	**CBS 128313**	*Vitis vinifera*	USA	HQ288227	HQ288269	HQ288306
	UCD 2604MO	*Vitis vinifera*	USA	HQ288228	HQ288270	HQ288307
Lasiodiplodia vitis	CBS 124060	*Vitis vinifera*	Italy	KX464148	KX464642	KX464917

[1] ATCC: American Type Culture Collection, Virginia, USA; BL: Personal number of B.T. Linaldeddu; Bot: Personal number of S. Denman; CBS: CBS-KNAW Fungal Biodiversity Centre, Utrecht, The Netherlands; CFCC: China Forestry Culture Collection Center, Beijing, China; CGMCC: China General Microbiological Culture Collection Center; CMM: Culture Collection of Phytopathogenic Fungi "Prof. Maria Menezes", Universidade Federal Rural de Pernambuco, Recife, Brazil; CMW: Tree Pathology Co-operative Program, Forestry and Agricultural Biotechnology Institute, University of Pretoria, South Africa; CPC: Working collection of P.W. Crous, housed at CBS; DAR: Plant Pathology Herbarium, Orange Agricultural Institute, Forest Road, Orange. NSW 2800, Australia; FAU: culture collection of Systematic Mycology and Microbiology Laboratory, USDA-ARS, Beltsville, Maryland, USA; GZCC: Guizhou Academy of Agricultural Sciences Culture Collection, GuiZhou, China; ICMP: International Collection of Microorganisms from Plants, Landcare Research, Aukland, New Zealand; IRAN: Iranian Fungal Culture Collection, Iranian Research Institute of Plant Protection, Iran; MFLUCC: Mae Fah Luang University Culture Collection, Chiang Rai, Thailand; STE-U: Culture collection of the Department of Plant Pathology, University of Stellenbosch, South Africa; UCD: University of California, Davis, Plant Pathology Department Culture Collection; UCR: University of California, Riverside. Sequences generated in this study indicated in *italics*. Ex-type isolates are indicated in bold font. [2] ITS: internal transcribed spacers 1 and 2 together with 5.8S nrDNA; *tef1*: translation elongation factor 1-α gene; *tub2*: beta-tubulin gene.

2.5. Effect of Temperature on Mycelial Growth

Six representative isolates (CVG 1929 and CVG 1930 for *Lasiodiplodia* spp., CVG 1937, CVG 1938, CVG 2045, and CVG 2046 for *Diaporthe* spp.) were selected and grown on PDA-S at 25 ± 1 °C for 7 days in the dark. Mycelial plugs (5 mm diameter) were taken from actively growing colonies, placed onto new PDA-S plates, and incubated at 5, 10, 15, 20, 25, 30, and 35 °C in the dark. The two perpendicular diameters of the same colonies were measured using a scale ruler from 3 to 5 days after inoculation, depending on the mycelial growth of each isolate. The radial growth rate (mm day^{-1}) was calculated from the obtained mean data. Ten replicate plates per isolate and temperature combination were considered in a completely randomized design. A nonlinear adjustment of the data was applied for each isolate through the generalized Analytis Beta model [69] to assess the variation in mycelial growth rate over temperature [70]. The average growth rates for each isolate and temperature were adjusted to a regression curve to estimate the minimum, maximum, and optimum growth temperature, along with the maximum growth rate (MGR) [70].

2.6. Pathogenicity Tests

2.6.1. Pathogenicity on Fruit

Five representative isolates of Botryosphaeriaceae (CVG 1930, CVG 1945, CVG 1980, CVG 2155, CVG 2160) and four representative isolates of *Diaporthe* spp. (CVG 2045, CVG 2046, CVG 1937, CVG 1938) were used for pathogenicity test on fruit. The selected isolates were the only ones able to produce conidia on PNA or MEA among all the others. The isolates were inoculated on wounded fruit of *C. sinensis* cv. Valencia. The trial was conducted using three replicates of 15 fruit for each tested isolate. Fruit were washed, surface disinfected by immersion in 2% sodium hypochlorite for 5 min and rinsed twice in sterile distilled water for 5 min, then dried on absorbent paper. The pedicel was removed, and each fruit was wounded with a sterile needle at the stem-end, as conducted by Aiello et al. [71] and Huang et al. [28]. A single inoculation was performed at the stem-end for each fruit with 20 µL of conidial suspension (10^5 conidia mL^{-1}). Conidial suspensions were prepared for each isolate by adding 10 mL of SDW to 7-year-old cultures growth on PDA-S, scraping the mycelia then filtering through muslin cloth. Control fruit were inoculated with 20 µL of SDW. After inoculation, fruit were placed in plastic boxes containing filter paper with SDW and covered with plastic bags, which were removed after 2 days. Fruit were incubated at 25 ± 1 °C with 12 h photoperiod. After 10 days, symptoms development was evaluated measuring two perpendicular diameters of the necrotic lesions. To fulfill Koch's postulates, re-isolation was performed using the same procedure described above. The obtained colonies were identified through the assessment of morphological and molecular characteristics.

2.6.2. Pathogenicity on Plants

Two representative isolates of Botryosphaeriaceae (CVG 1929 and CVG 1985) and two isolates of *Diaporthe* spp. (CVG 1938, CVG 2046) were selected among the isolates found in association with citrus twigs for pathogenicity tests on plants. Their capacity to infect wood and induce twig blight was evaluated on two-year-old potted plants of *C. sinensis* cv. Valencia. Each fungal isolate was inoculated on six plants. For each plant, four twigs were inoculated as replicates. The inoculum consisted of a small piece (~5 mm) of mycelial plug from 5-day-old and 28-day-old cultures of isolates on PDA for *Lasiodiplodia* and for *Diaporthe* suspected isolates, respectively. The bark was first gently scraped using a sterile blade, and then the mycelial plug was inserted upside down onto the wound. Wounds were sealed with Parafilm (Bemis Co, Neenah, WI, USA) to prevent desiccation. Control consisted of sterile PDA mycelial plugs placed on bark wounds. All the inoculated plants were incubated in the growth chamber with a 12 h photoperiod and maintained at 25 ± 1 °C and regularly watered and monitored daily for development of symptoms. Disease incidence (%) and disease severity (lesion length cm) were evaluated 7 and

14 days post inoculations. Re-isolations were performed as mentioned above to fulfill Koch's postulates.

2.7. Statistical Analysis

The data obtained from the experiment conducted to evaluate the temperature effect on mycelial growth rate were subjected to statistical analysis as follows. Data of optimum growth temperature and MGR were evaluated for normality and homogeneity of residual variances. One-way ANOVA was performed when both ANOVA assumptions were satisfied for optimum growth temperature and MGR data. The optimum growth temperature or MGR was considered as a dependent variable, and isolates were considered as independent variables. For each variable, isolate means were compared according to Tukey's honestly significant difference (HSD) test at $\alpha = 0.05$ [72]. Data were analyzed using Statistix 10 software [73]. Data obtained from pathogenicity tests on fruit and plants were subjected to statistical analysis to assess the aggressiveness of the tested isolates. Considering fruit, as the two obtained perpendicular diameters of necrotic lesions on fruit have different lengths, the mathematical formula for elliptic surface was used to calculate the necrotic lesion areas induced by inoculated isolates [74]. Necrotic areas were compared and analyzed using RStudio (https://www.R-project.org/ accessed on 1 November 2023). Normality and homogeneity of residual variances were evaluated with Shapiro–Wilk and Levene's tests, respectively. One-way analysis of variance (ANOVA) was carried out to compare the average of necrotic areas among the different species and the control. Bonferroni post hoc test (at $p < 0.05$) was used to evaluate statistically significance differences in means of necrotic area surface. For plants, the frequency of branch dissection was calculated based on the numbers of dissected branches recorded. Data were analyzed using RStudio (https://www.R-project.org/ accessed on 1 November 2023). Shapiro–Wilk and Levene's tests were used to evaluate normality and homogeneity of residual variances, respectively. To compare the frequency of branches dissection among isolates, ANOVA was carried out. Bonferroni post hoc test (at $p < 0.05$) was used to determine statistically significant differences.

3. Results

3.1. Field Sampling and Isolation

In the 35 sampled Florida orchards, dieback and stem-end rot seriously reduced the plant health and fruit yield, respectively. Citrus trees showed a wide variety of symptoms, including twig and branch dieback often associated with gummosis exudate (Figure 2c,d). Branch and twig longitudinal sections revealed necrotic brown discoloration. Necrotic lesions at the stem-end were observed on green and ripe fruit. Green fruit showed yellowing at the stem-end, while ripe fruit exhibited brown necrotic tissue, and in both cases, a brown rot occurred at the calyx end (Figure 2a,b). A total of 70 fungal isolates were obtained from sampled orchards. The preliminary identification of collected isolates was based on morphology. Fifty-five isolates were identified as Botryosphaeriaceae-like and 15 as *Diaporthe* spp. Twenty-six representative isolates were selected for molecular analysis.

3.2. Phylogenetic Analyses

Three alignments representing single locus analyses of ITS, *tef1*, and *tub2* and one combined alignment of all three loci were analyzed for Botryosphaeriaceae and *Diaporthe* isolates. The three single loci alignments produced topologically similar trees. The combined locus phylogeny of Botryosphaeriaceae consisted of 82 sequences, including the outgroup *Dothiorella viticola* (CBS 117009). The analyses included a total of 1356 characters (ITS:1-493, *tef1*:498-899, *tub2*:904-1,356). For the Bayesian analyses, MrModeltest suggested the fixed state frequency for analyzing ITS, Dirichlet state frequency for *tef1* and Dirichlet, and fixed state frequencies for *tub2*. Based on the results of MrModeltest, the following models were adopted: K80 + G and K80 + I for ITS, K80 + G and HKY + I + G for *tef1*, and GTR + I and GTR + G for *tub2*. In the Bayesian analyses, the ITS had 98 unique site patterns,

while the partial *tef1* gene had 113, and the partial *tub2* gene had 99. The analyses ran for 37,535,000 generations, resulting in 75,072 trees, of which 56,304 trees were used to calculate the posterior probabilities. Considering the concatenated phylogenetic analyses, twenty-two isolates clustered with 11 reference strains and the ex-type of *Lasiodiplodia iraniensis*, forming a highly supported clade (0.9/100). Regarding the MP analysis, 216 characters resulted as parsimony-informative, 219 were variables, and 1219 were constant. A maximum of 1000 equally most parsimonious trees were saved (Tree length = 427, CI = 0.806, RI = 0.845, and RC = 0.681). Bootstrap support values obtained with the parsimony analyses are reported on the Bayesian phylogenetic tree (Figure 3).

The *Diaporthe* multi-locus phylogenetic analyses consisted of 44 sequences, including the outgroup *D. corylina* (CBS 121124). The phylogenetic analyses included a total of 1.726 characters (ITS:1-552, *tef1*:557-880, *tub2*:885-1726). For the Bayesian analyses, MrModeltest proposed the fixed state frequency distributions for analyzing ITS and Dirichlet state frequency for *tef1* and *tub2*. In line with MrModeltest's recommendations, the following models were used: SYM + I + G for ITS, GTR + I + G, and HKY + I + G for *tef1* and K80 + G and HKY + G for *tub2*. In the Bayesian analyses, the ITS had 156 unique site patterns, the partial *tef1* gene had 245, and the *tub2* locus had 415. The analyses ran for 720,000 generations, resulting in 1442 trees, of which 817 trees were used to calculate the posterior probabilities. For the MP analysis, 590 characters resulted as parsimony-informative, 415 were variable, and 713 were constant. A maximum of 1000 equally most parsimonious trees were saved (Tree length = 2.271, CI = 0.661, RI = 0.854, and RC = 0.564). Bootstrap support values obtained with the parsimony analyses are reported on the Bayesian phylogenetic tree (Figure 4). Considering the combined analyses, two isolates clustered with one reference strain and the ex-type of *Dia. ueckerae*, while two isolates clustered with the ex-type of *Dia. pseudomangiferae* forming a highly supported clade (1/100).

3.3. Morphology

Morphological characteristics, supported by phylogenetic analysis, were used to describe the three identified species.

L. iraniensis was characterized by a cottony, fast-growing colony with abundant aerial mycelium, which covered the entire PDA-S Petri dishes after 7 days (Figure 5a,b). Initially, the colony was white or light gray and then became smoke-grey to olivaceous-grey (Figure 5a). The reverse colony was white or pale grey which turned later to dark grey or greenish grey (Figure 5b). On PNA, *L. iraniensis* produced pycnidial, dark brown to black conidiomata covered with dense mycelium. Initially, conidia were hyaline, subglobose to ovoid, unicellular with granular content, becoming dark brown, ovoid to ellipsoid, and 1-septate with longitudinal striations (Figure 5c). Mature conidia of the strains CVG 1930, CVG 1945, CVG 1980, CVG 2155, and CVG 2160 had dimensions of (20.1-) 24.2 (-29.2) × (13.8-) 14.6 (-16.3) µm (mean ± SD = 24.2 ± 1.5 × 14.6 ± 1.0 µm).

Dia. ueckerae showed a dense and felt-like colony that covered the PDA-S plates within 10 days. Front colony was white, becoming cream to pale grey (Figure 5d). The reverse colony was white, turning to grey with brownish spots (Figure 5e). On MEA, the strains CVG 1937 and CVG 1938 of *Dia. ueckerae* produced pycnidial, subglobose dark brown to black conidiomata. Alpha conidia were aseptate, hyaline, smooth, fusiform, and apex rounded (Figure 5f), with size of (5.4-) 8.3 (-9.2) × (2.3) 3.5 (-4.5) µm (mean ± SD = 8.3 ± 1.0 × 3.5 ± 0.8 µm). Beta conidia were aseptate, hyaline, smooth, filiform, curved, and eguttulate (Figure 5f) with dimensions of (17.3-) 21.4 (-24.3) × (1.0-) 1.5 (2.5) µm (mean ± SD = 21.4 ± 1.5 × 1.5 ± 0.4 µm).

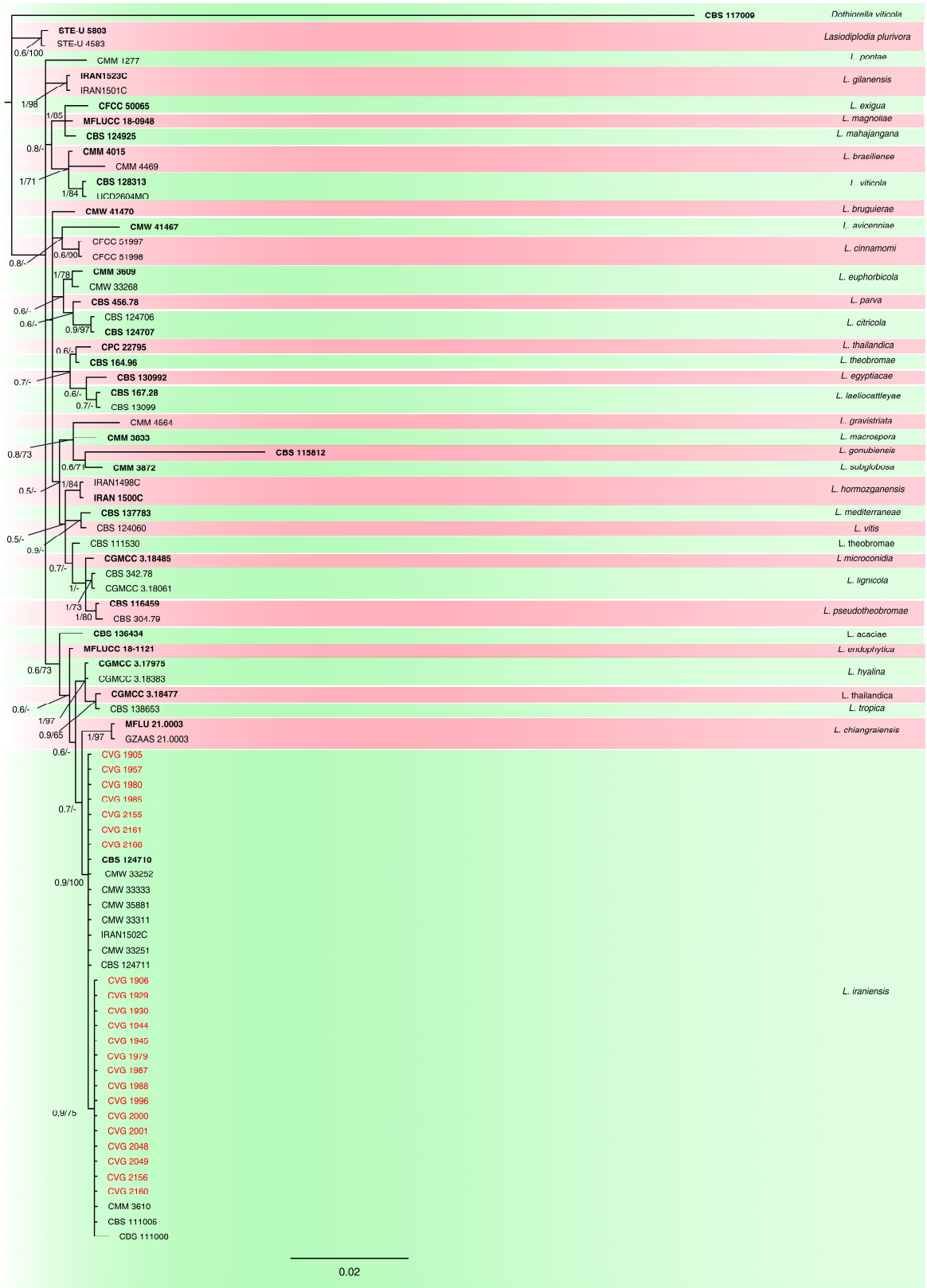

Figure 3. Phylogenetic tree of *Lasiodiplodia* spp., resulting from a Bayesian analysis of the combined ITS, *tef1*, and *tub2* sequence alignment. Bayesian posterior probabilities (PP) and Maximum likelihood bootstrap support values (ML-BS) are reported at the nodes (PP/MLBS). Ex-type strains are indicated in bold, and species are delimited with colored blocks. The isolates collected in the present study are indicated in red. The tree was rooted to *Dothiorella viticola* (CBS 117009).

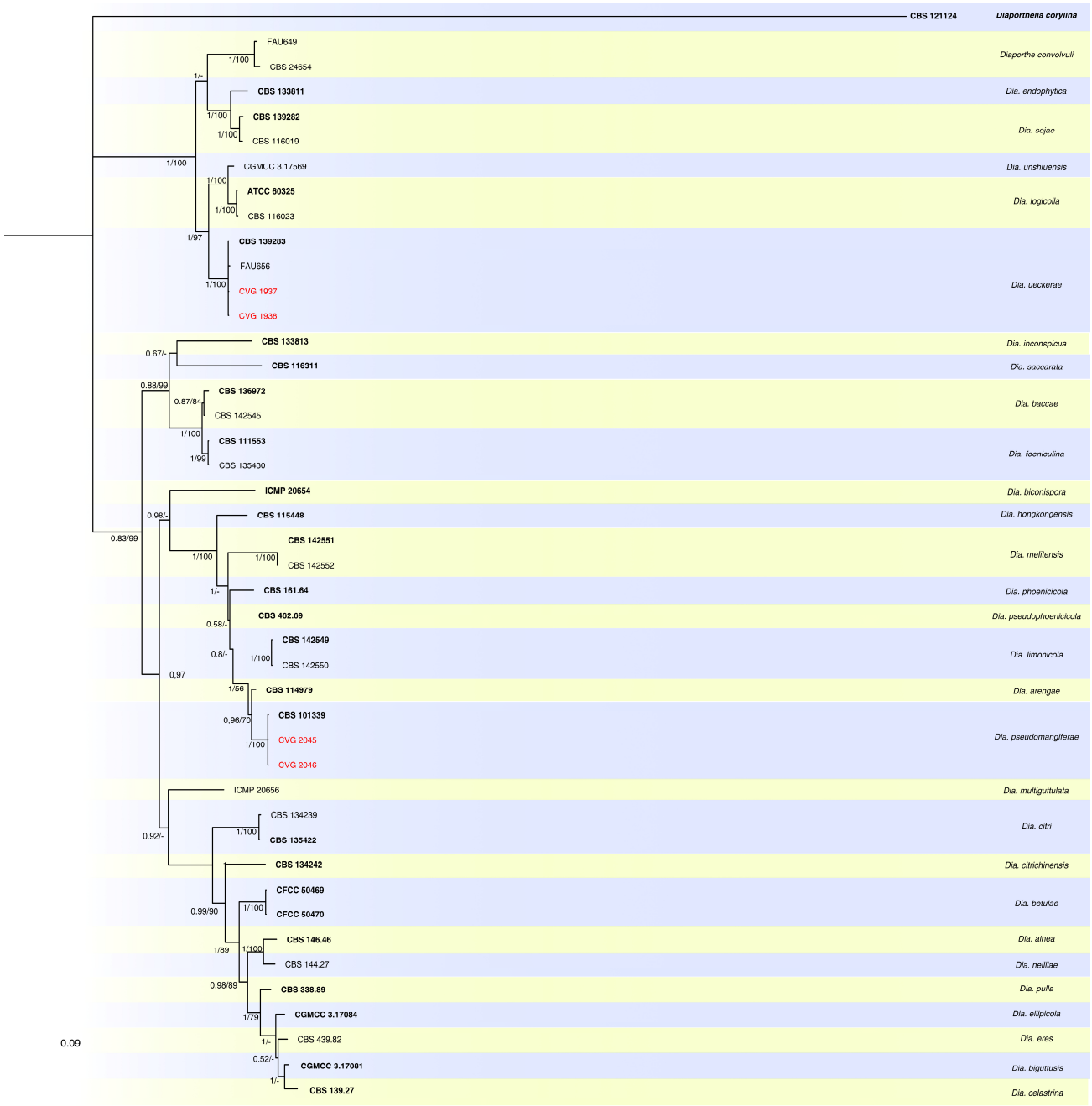

Figure 4. Phylogenetic tree of *Diaporthe* spp., resulting from a Bayesian analysis of the combined ITS, *tef1*, and *tub2* sequence alignment. Bayesian posterior probabilities (PP) and Maximum likelihood bootstrap support values (ML-BS) are reported at the nodes (PP/MLBS). Ex-type strains are indicated in bold, and species are delimited with colored blocks. The isolates collected in the present study are indicated in red. The tree was rooted to *Diaporthella corylina* (CBS 121124).

Dia. pseudomangiferae had white moderate aerial mycelia with patches from pale luteous to luteous (yellowish or yellow-brown) in reverse (Figure 5g,h). Superficial, pycnidial, and black conidiomata were produced on MEA by the strains CVG 2045 and CVG 2046. Alpha conidia were aseptate, hyaline, smooth, and fusiform (Figure 5i) with a size of (4.2-) 7.3 (-11.0) × (1.3) 2.5 (-3.5) µm (mean ± SD = 7.3 ± 1.2 × 2.5 ± 1.1 µm). Beta conidia were aseptate, hyaline, smooth, and curved (Figure 5i) with dimensions of (14.5-) 25.4 (-30.4) × (1.3-) 1.3 (2.3) µm (mean ± SD = 25.4 ± 1.3 × 1.3 ± 1.0 µm).

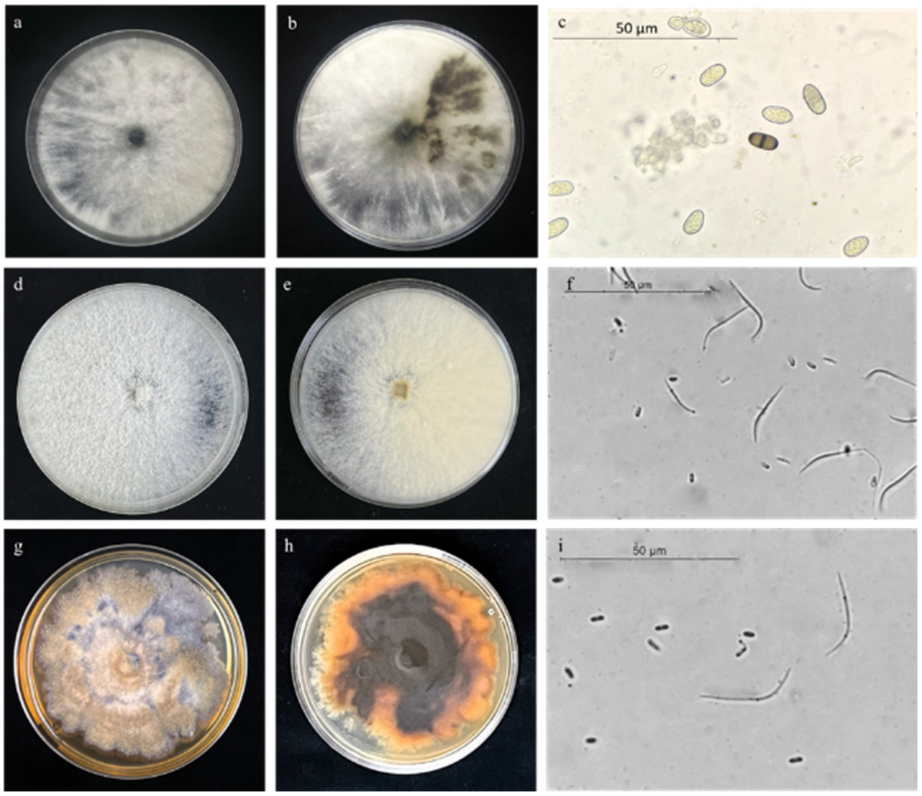

Figure 5. Morphological characteristics of the front and reverse sides of colonies and the conidia of the different fungal species grown on PDA-S. (**a**–**c**) *Lasiodiplodia iraniensis*; (**d**–**f**) *Diaporthe ueckerae*; (**g**–**i**) *Diaporthe pseudomangiferae*.

3.4. Effect of Temperature on Mycelial Growth

All the selected isolates were able to grow from 10 to 35 °C, while no mycelial growth was recorded at 5 °C in all cases. No significant differences were found in optimum growth temperature and MGR ($p > 0.05$) among isolates. However, there was a significant interaction among isolates and species in optimum growth temperature ($p < 0.05$); thus, the data were not combined, and isolates were kept separate for both the analyses on optimum growth temperature and MGR (Figure 6, Table 3). The optimum growth temperature ranged from 26.0 to 28.4 °C for *Dia. ueckerae* isolate CVG 1938, and *L. iraniensis* isolate CVG 1929, respectively.

Table 3. Effect of temperature on mycelial growth of representative fungal isolates selected in this study, grown on PDA at 5, 10, 15, 20, 25, 30, and 35 °C in the dark from 4 to 7 days [(1)].

Family/Fungal Species	Isolate	Analytis Beta Model [(2)]			Temperature (°C) [(3,5)]			MGR (mm day^{-1}) [(4,5)]
		R^2	a	b	Optimum	Minimum	Maximum	
Lasiodiplodia iraniensis	CVG 1929	0.9927	2.65	0.78	28.4 a	4.0	35.5	13.7 a
	CVG 1930	0.9924	3.42	1.13	28.1 a	4.0	36.0	13.8 a
Diaporthe pseudomangiferae	CVG 2045	0.8474	4.20	2.19	26.7 b	5.0	38.0	4.5 c
	CVG 2046	0.8675	3.64	1.74	27.2 bc	4.5	38.0	4.5 c
Diaporthe ueckerae	CVG 1937	0.9257	4.11	2.00	26.2 cd	4.0	37.0	6.3 b
	CVG 1938	0.9774	4.20	2.05	26.0 d	4.5	36.5	6.1 b

[(1)] Data represent the average of five replicated Petri dishes per isolate and temperature combination; [(2)] Analytis Beta model, where R^2 = coefficient of determination, and a, b = coefficients of regression; [(3)] For each isolate, temperature average growth rates were adjusted to a regression curve to estimate the minimum, maximum and optimum growth temperature; [(4)] MGR: Maximum growth rate (mm per day) obtained by the Analytis Beta model at the optimum growth temperature; [(5)] Means in a column followed by the same letter do not differ significantly according to Tukey's HSD test at $p = 0.05$ applied to untransformed optimum growth temperature data and log-transformed MGR data [70].

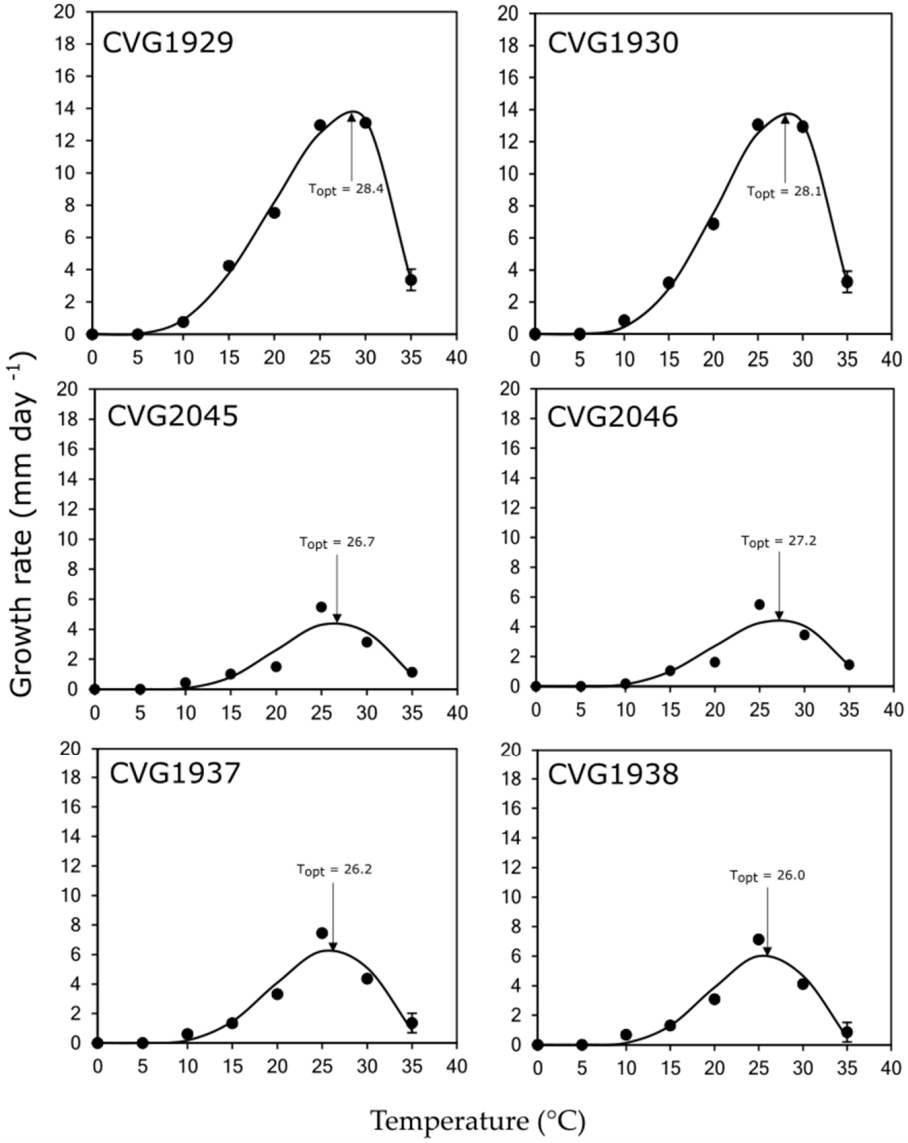

Figure 6. Effect of temperature on mycelial growth rate (mm day^{-1}) of the 6 representative isolates selected in this study grown on PDA-S at 5, 10, 15, 20, 25, 30, and 35 °C in the dark for 3 to 5 days. Average growth rates over temperature were adjusted for each isolate to a nonlinear regression curve through the Analytis Beta model. Data points represent the means of ten replicated plates each. Vertical bars represent the standard error of the means. CVG 1929, CVG 1930—*Lasiodiplodia iraniensis*. CVG 2045, CVG 2046—*Diaporthe pseudomangiferae*. CVG 1937, CVG 1938—*Diaporthe ueckerae*.

Concerning the MGR, isolates belonging to *L. iraniensis* had the highest mycelial growth, with MGR being 13.7–13.8 mm day^{-1}, followed by isolates of *Dia. ueckerae* (MGR = 6.1–6.3 mm day^{-1}). Isolates belonging to *Dia. pseudomangiferae* showed the lowest MGR with respect to the other isolates, with MGR being 4.5 mm day^{-1}.

3.5. Pathogenicity on Fruit

Dia. pseudomangiferae, *Dia. ueckerae* and *L. iraniensis* produced soft, watery rot at the stem-end of inoculated fruit of *C. sinensis* cv. Valencia. Discoloration started from the button where the fruit were wounded, and the conidia suspension was added. Ten days after inoculation, lesions extended to the whole fruit, producing a rot (Figure 7d–f).

Figure 7. Pathogenicity tests of selected *L. iraniensis*, *Dia. pseudomangiferae* and *Dia. ueckerae* isolates on *Citrus sinensis* cv. Valencia two-year-old potted plants and fruit. (**a**) 'Valencia' plant inoculated with *Dia. pseudomangiferae*: (**b**) inoculation point with abundant gummosis of 'Valencia' plant caused by *L. iraniensis*; (**c**) twig dieback of 'Valencia' plant caused by *L. iraniensis*; (**d**) stem-end rot on 'Valencia' fruit inoculated by *Dia. pseudomangiferae*; (**e**) stem-end rot on 'Valencia' fruit inoculated by *Dia. ueckerae*; (**f**) stem-end rot on 'Valencia' fruit inoculated by *L. iraniensis*.

The isolates of *L. iraniensis* produced the largest necrotic area compared to both species of *Diaporthe* spp. and the water control (Figure 8). The isolate CVG 2160 was the most virulent, producing a necrotic area of 233 cm^2 (Figure 8). The other *L. iraniensis* isolates showed different virulence levels, ranging from 175 cm^2 to 216 cm^2 for the strains CVG 2155 and CVG 1930, respectively (Figure 8). Isolates of *Dia. pseudomangiferae* showed a higher virulence than those of *Dia. ueckerae*. In particular, isolates CVG 2045 and CVG 2046 of *Dia. pseudomangiferae* produced a mean necrotic area of 72 cm^2 and 27 cm^2, respectively (Figure 8). While isolates of *Dia. ueckerae*, CVG 1937, and CVG 1938 were able to produce necrotic lesions, with mean areas of 20 cm^2 and 7 cm^2, respectively (Figure 8). No symptoms were observed on water control fruit. All the fungal species were successfully re-isolated from the outer margin of necrotic tissues of inoculated fruit, fulfilling Koch's postulates. The recovery of inoculated isolates of species ranged between 80% and 90%. The identity of the re-isolated isolates was confirmed through morphological features and molecular analyses of the *tub2* locus.

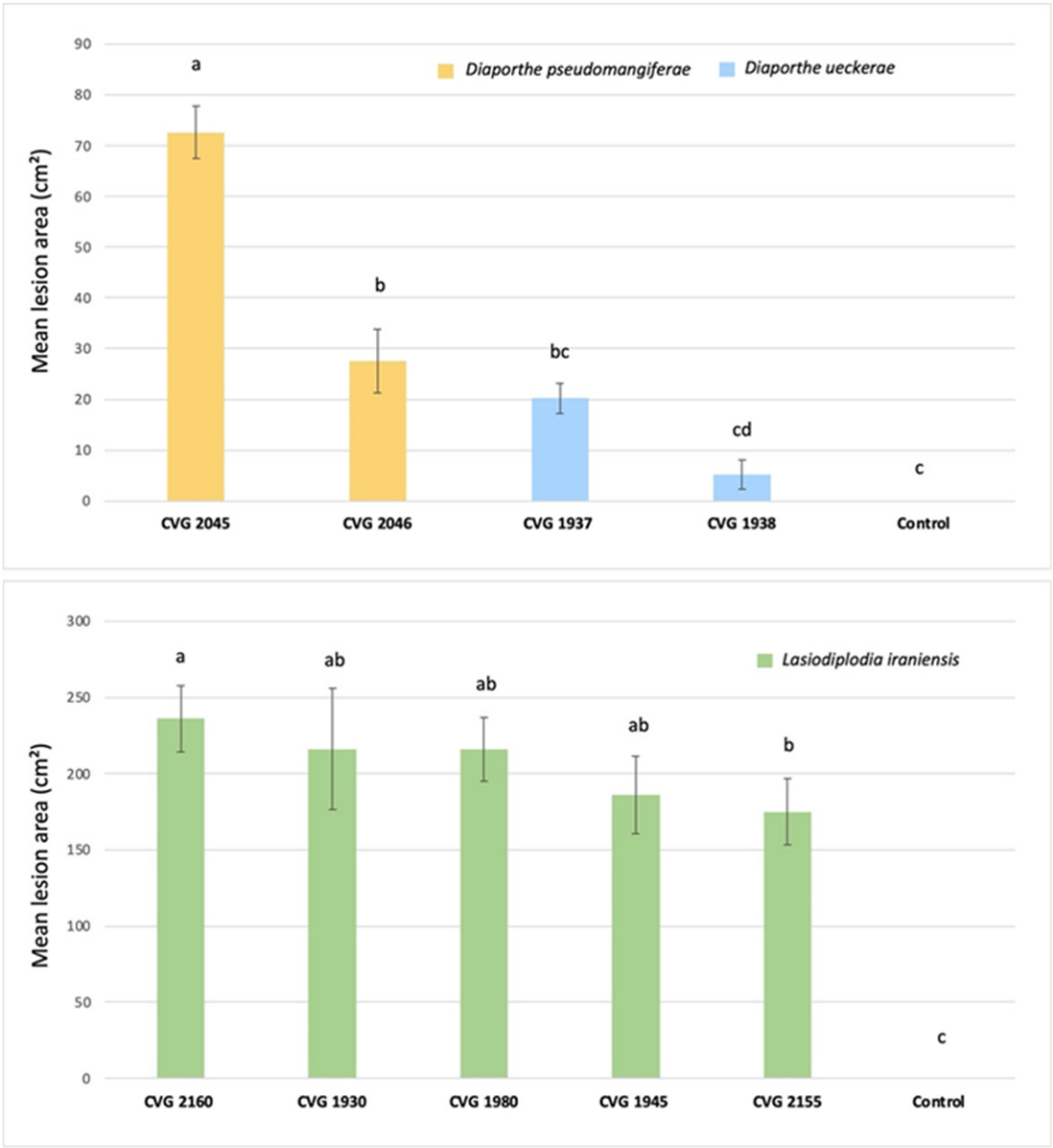

Figure 8. Mean lesion area (in cm^2) on inoculated fruit of *C. sinensis* cv. Valencia, obtained from diameters measured 10 days after inoculation with conidia suspension at 1×10^5 cfu/mL. Means in each histogram indicated by different letters are significantly different ($p < 0.05$) according to the Bonferroni *post hoc* test. Vertical bars indicate standard error of the mean. Data from each pathogenicity test were analyzed separately.

3.6. Pathogenicity on Plants

Two tested isolates of *L. iraniensis* (CVG 1929 and CVG 1985) and the isolate CVG 2046 of *Dia. pseudomangiferae* were able to cause necrotic lesions and gummosis at the inoculation point after 7 days (Figure 7b), while a complete twig decay occurred after 14 days (Figure 7a,c). Plants inoculated with the isolate CVG 1938 of *Dia. ueckerae* showed no symptoms, as control plants. Tested isolates of *L. iraniensis* showed a high level of virulence: CVG 1929 produced 73% of decayed twigs on a total number of 24 plants inoculated, followed by CVG 1985 with 67% (Figure 9). The tested isolate of *Dia. pseudomangiferae* (CVG 2046) caused 38% of decayed twigs, showing lower virulence compared to *L. iraniensis* isolates (Figure 9).

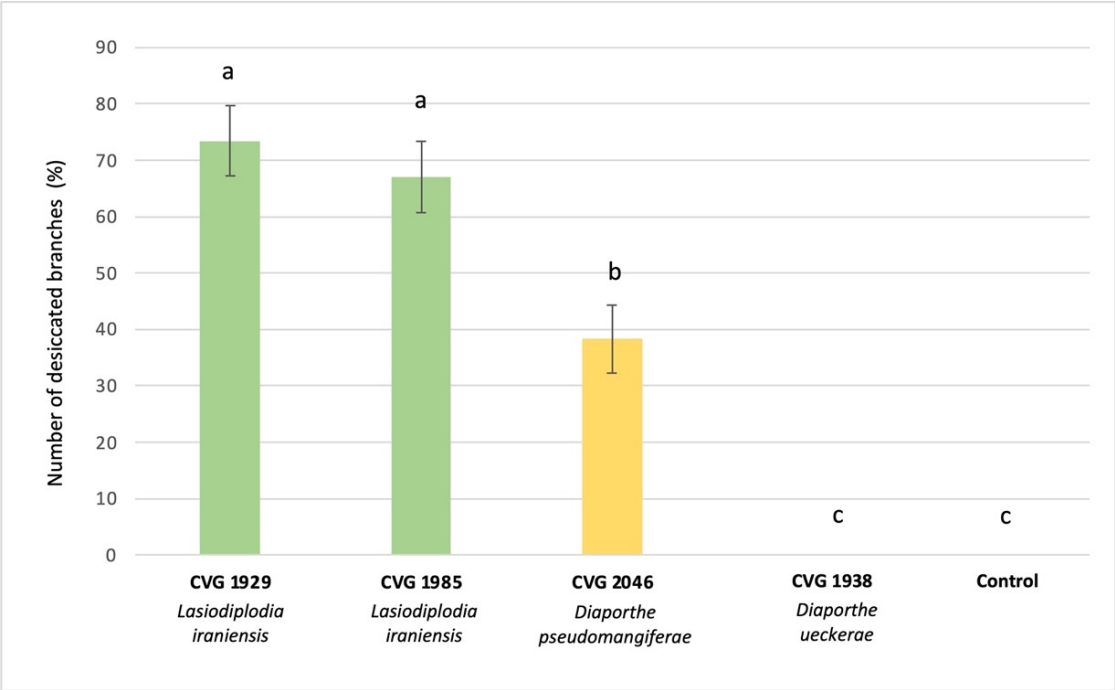

Figure 9. Numbers of desiccated branches expressed as percentage on a total of 24 branches inoculated with mycelial plug (~5 mm) from two-year-old potted plants of *C. sinensis* cv. Valencia. Means in each histogram indicated by different letters are significantly different ($p < 0.05$) according to Bonferroni *post hoc* test. Vertical bars indicate standard error of the mean.

4. Discussion

The present study is the first that aimed at revealing the occurrence, diversity, and pathogenicity of fungal species in association with twig blight, branch dieback, fruit rot, and decline of *C. sinensis* cv. Valencia in Florida. Severe symptoms of dieback and stem-end rot were observed on branches, twigs, and fruit in several orchards across South-central Florida. Different fungal isolates were recovered from plant material samples collected in 35 orchards and they were preliminary identified as Botryosphaeriaceae-like and *Diaporthe*-like according to their colony morphology [30,39,75]. We identified for the first time three different species as the main causal agents of this disease: *L. iraniensis*, *Dia. pseudomangiferae*, and *Dia. ueckerae*.

Lasiodiplodia iraniensis was described in 2010 as a new species in association with *Citrus* sp., *Juglans* sp., and *Mangifera indica* in Iran [76]. Later, this pathogen was reported on cashews, *Anacardium occidentale* [77], great bougainvillea, *Bougainvillea spectabilis* [78], gum trees, *Eucalyptus* spp. [79], mango, *Mangifera indica* [80,81], and toothbrush tree, *Salvadora persica* [76]. Concerning citrus, it was reported in association with dieback disease on key lime, *C. aurantiifolia* in Oman [80], Persian lime, *C. latifolia* in Mexico [33] and mandarin, *C. reticulata* in Pakistan, where it was found in association with *Colletotrichum siamense* [82]. Recently, *L. mitidjana* was reported on *C. sinensis* in Algeria, causing branch canker and dieback [16]. To our knowledge, this study is the first report of *L. iraniensis* as a causal agent of dieback and stem-end rot diseases on *C. sinensis* worldwide. Other *Lasiodiplodia* spp. reported to cause stem-end rot on *Citrus* spp. are *L. theobromae* [24] and *L. pseudotheobromae* [37,83].

Diaporthe ueckerae is a ubiquitous pathogen that opportunistically infects humans and plants [46]. It was described for the first time by Udayanga et al. [46] on *Cucumis* sp. and then reported on peanut, *Arachis hypogaea* [84], tea plant, *Camellia sinensis* [85], lemon-scented gum, *Eucalyptus citriodora* [86], soybean, *Glycine max* [87], white-fleshed pitahaya, *Selenicereus undatus* [88], and mango, *M. indica* [25]. *Diaporthe pseudomangiferae* is a plant pathogen first described by Gomes et al. [39] and isolated from mango [89,90],

cacao, *Theobroma cacao* [89,91], and kiwifruit *Actinidia deliciosa* [92]. It was reported in Puerto Rico, California, the Dominican Republic, Mexico, China, and South Korea [39,89–92]. To our knowledge, *Dia. pseudomangiferae* and *Dia. ueckerae* are reported in this study for the first time in association with citrus dieback diseases and stem-end rot worldwide. Other *Diaporthe* species are reported as causal agents of pre- or post-harvest diseases on citrus: *Dia. citri*, *Dia. foeniculina*, *Dia. limonicola*, and *Dia. melitensis* [7,19,28].

We show that all the tested isolates have an optimum growth temperature in a range between 26.0 and 28.4 °C with different MGR based on the species, in agreement with other reports [32,93]. Climate conditions in the majority of Florida are reported as humid subtropical (Cfa Köppen climate type) with higher temperature and humidity in summer and warm, occasionally cold, dry winters, thus being suitable for the development and spread of these pathogens [94]. Moreover, isolates belonging to *L. iraniensis* had both the highest optimum growth temperature and MGR with respect to the other tested species. In general, species of *Lasiodiplodia* are well adapted to places with higher annual mean temperatures, and Botryosphaeriaceae are known as fast-growing fungi [32,95,96]. The present in vitro findings suggest that *L. iraniensis* could have a greater colonization ability on the host plant tissues. Thus, further investigations will aim to assess the *in planta* development of these pathogens on mature trees depending on temperature conditions and the possible effect of temperature on disease severity to predict and model the disease progress.

Concerning the pathogenicity, the tested isolates of *L. iraniensis* were able to cause soft, watery stem-end rot when inoculated on citrus fruit, and they were more virulent in comparison to the other tested fungal species. This outcome is consistent with the results reported by Li et al. [97] on mango, where *L. iraniensis* was the most virulent species along with *Botryosphaeria scharifii*. The different virulence levels found among *L. iraniensis* isolates suggest a possible intraspecific variability that could be addressed in future studies. We suspect that opportunistic strains of this fungal species requiring plant stresses, like drought, as the preconditioning factor to allow infection establishment could exist, potentially explaining the variable virulence levels we detected. For example, a relatively closely related species, *Botryosphaeria dothidea*, is a well-known opportunistic pathogen of various tree species, including apple [98] and coast redwood, requiring drought stress to infect wood [99–101]. A pathogenicity test conducted on potted *C. sinensis* plants cv. Valencia confirmed *L. iraniensis* as the most virulent species, able to cause more than 70% of completely decayed twigs of young plants. The obtained reslts agree with previous studies conducted on this species affecting citrus trees: Xiao et al. [36] reported *Lasiodiplodia* as the most virulent genus on *C. reticulata* shoots and on *C. paradisi* × *C. reticulata* plants in China, while Bautista-Cruz et al. [33] described *L. iraniensis* as one of the most virulent species on Persian lime, *C. latifolia*, plants in Mexico. Similar results were also reported on dragon fruit, *S. undatus*, cashews, *Anacardium*, and macadamia nut, *Macadamia integrifolia* [77,102,103]. Considering *Dia. pseudomangiferae*, the tested isolates were pathogenic on both fruit and plants, while for *Dia. ueckerae*, the isolates were pathogenic only on fruit. The symptoms caused by the isolate CVG 1938 of *Dia. ueckerae* on fruit were statistically similar to the water control; thus, it is possible that it was not able to cause symptoms on wood because it is either a more complex matrix or an unsuitable ecological niche overall. In this case, it is also possible that *Dia. ueckerae* might require some form of plant stress as the prerequisite to infect *C. sinensis* wood. Further inoculation studies of *Dia. ueckerae* on well-watered plants vs. drought-stressed plants will provide clearer information on its pathogenicity.

Several studies demonstrated a positive correlation between different citrus diseases and the early drop of fruit [104–107]. Thus, considering *L. iraniensis*, *Dia. ueckerae*, and *Dia. pseudomangiferae* as causal agents of dieback disease and stem-end rot, a possible role of these species as biotic factors contributing to the early drop of citrus fruit in the sampled area is postulated, but further studies are needed to investigate this aspect. Furthermore, the physiological status of the sampled trees indicating the presence or absence of plant stress, with a special focus on drought, might be an important aspect in these

investigations. Additional assays on wood and fruit co-infection with the identified fungal species will provide useful information about their role in the development and progress of the mentioned disease. Moreover, Botryosphaeriaceae and *Diaporthe* spp. are reported to infect plants mainly through natural openings or wounds [108,109]. Different cultural practices, such as pruning and fruit thinning, could cause wounds on plants, thus favoring the entry of these pathogens and subsequent development of dieback and stem-end rot. Optimal management of orchards and the protection of wound cuts is recommended to avoid the spread of these pathogens. Future investigations on the ecology, epidemiology, and sensitivity of fungicides labeled for use in Florida will improve the knowledge about these pathogens to develop effective management strategies. In this context, the role of irrigation and nutrient balance in plant health should be explored as a possible way to prevent stress conditions which could make the plants less vulnerable to the pathogens identified and characterized in this study.

Supplementary Materials: The following supporting information can be downloaded at: https://www.mdpi.com/article/10.3390/horticulturae10040406/s1, Table S1: Collection details and of isolates of this study.

Author Contributions: Conceptualization, M.F. and V.G.; methodology, V.P., M.F. and D.A.; software, I.M.; validation, S.G.A., D.S. and V.G.; formal analysis, G.D. and I.M.; investigation, V.P., M.F. and V.G.; resources, M.F.; data curation, V.P. and V.G.; writing—original draft preparation, V.P.; writing—review and editing, D.S, G.P. and V.G.; visualization, V.G.; supervision, V.G.; project administration, V.G.; funding acquisition, V.G. All authors have read and agreed to the published version of the manuscript.

Funding: This research was funded by KeyPlex. Part of this work was granted by the European Commission—NextGenerationEU, Project "Strengthening the MIRRI Italian Research Infrastructure for Sustainable Bioscience and Bioeconomy", code n. IR0000005.

Data Availability Statement: The raw data supporting the conclusions of this article will be made available by the authors on request.

Conflicts of Interest: Author Mauricio Flores was employed by the company KeyPlex, 400 N. New York Ave Suite 200, Winter Park, FL 32789, USA. The remaining authors wish to disclose that, at the time of conducting this research and submitting the manuscript, they were not subject to any commercial or financial relationships that could be perceived as a potential conflict of interest.

References

1. Rehman, S.U.; Abbasi, K.S.; Qayyum, A.; Jahangir, M.; Sohail, A.; Nisa, S.; Tareen, M.N.; Tareen, M.J.; Sopade, P. Comparative analysis of citrus fruits for Nutraceutical properties. *Food Sci. Technol.* **2020**, *40*, 153–157. [CrossRef]
2. ISTAT. Istituto Nazionale di Statistica. 2023. Available online: https://www.istat.it/ (accessed on 1 November 2023).
3. FAOSTAT. Food and Agriculture Organization Corporate Statistical Database. 2023. Available online: https://www.fao.org (accessed on 20 December 2023).
4. USDA. United States Department of Agriculture. 2023. Available online: https://www.usda.gov (accessed on 20 December 2023).
5. Timmer, L.W.; Garnsey, S.M.; Graham, J.H. *Compendium of Citrus Diseases*; American Phytopathology Society: Saint Paul, MN, USA, 2000.
6. Bezerra, J.D.P.; Crous, P.W.; Aiello, D.; Gullino, M.L.; Polizzi, G.; Guarnaccia, V. Genetic Diversity and Pathogenicity of. *Plants* **2021**, *10*, 492. [CrossRef] [PubMed]
7. Chaisiri, C.; Liu, X.Y.; Lin, Y.; Luo, C.X. *Diaporthe citri*: A Fungal Pathogen Causing Melanose Disease. *Plants* **2022**, *11*, 1600. [CrossRef] [PubMed]
8. Galsurker, O.; Diskin, S.; Maurer, D.; Feygenberg, O.; Alkan, N. Fruit Stem-End Rot. *Horticulturae* **2018**, *4*, 50. [CrossRef]
9. Mayorquin, J.S.; Wang, D.H.; Twizeyimana, M.; Eskalen, A. Identification, Distribution, and Pathogenicity of Diatrypaceae and Botryosphaeriaceae Associated with Citrus Branch Canker in the Southern California Desert. *Plant Dis.* **2016**, *100*, 2402–2413. [CrossRef] [PubMed]
10. Vitale, A.; Aiello, D.; Azzaro, A.; Guarnaccia, V.; Polizzi, G. An Eleven-Year Survey on Field Disease Susceptibility of Citrus Accessions to *Colletotrichum* and *Alternaria* Species. *Agriculture* **2021**, *11*, 536. [CrossRef]
11. Fawcett, H.S.; Burger, O.F. A gum-inducing Diplodia of peach and orange. *Mycologia* **1911**, *3*, 151–153. [CrossRef]
12. Punithalingam, E. *Plant Diseases Attributed to Botryodiplodia Theobromae Pat*; J. Cramer.: Englewood Cliffs, NJ, USA, 1980.

13. Adesemoye, A.O.; Mayorquin, J.S.; Wang, D.H.; Twizeyimana, M.; Lynch, S.C.; Eskalen, A. Identification of Species of Botryosphaeriaceae Causing Bot Gummosis in Citrus in California. *Plant Dis.* **2014**, *98*, 55–61. [CrossRef] [PubMed]
14. Espargham, N.; Mohammadi, H.; Gramaje, D. A Survey of Trunk Disease Pathogens within Citrus Trees in Iran. *Plants* **2020**, *9*, 754. [CrossRef]
15. Crous, P.W.; Wingfield, M.J. Fungi infecting woody plants: Emerging frontiers. *Persoonia* **2018**, *40*, I–III. [CrossRef]
16. Berraf-Tebbal, A.; Mahamedi, A.E.; Aigoun-Mouhous, W.; Špetík, M.; Čechová, J.; Pokluda, R.; Baránek, M.; Eichmeier, A.; Alves, A. Lasiodiplodia mitidjana sp. nov. and other Botryosphaeriaceae species causing branch canker and dieback of Citrus sinensis in Algeria. *PLoS ONE* **2020**, *15*, e0232448. [CrossRef]
17. Camiletti, B.X.; Lichtemberg, P.S.F.; Paredes, J.A.; Carraro, T.A.; Velascos, J.; Michailides, T.J. Characterization of. *Phytopathology* **2022**, *112*, 1454–1466. [CrossRef]
18. Guarnaccia, V.; Groenewald, J.Z.; Polizzi, G.; Crous, P.W. High species diversity in *Colletotrichum* associated with citrus diseases in Europe. *Persoonia* **2017**, *39*, 32–50. [CrossRef] [PubMed]
19. Guarnaccia, V.; Crous, P.W. Emerging citrus diseases in Europe caused by species of. *IMA Fungus* **2017**, *8*, 317–334. [CrossRef] [PubMed]
20. Riolo, M.; Aloi, F.; Pane, A.; Cara, M.; Cacciola, S. Twig and Shoot Dieback of Citrus, a New Disease Caused by *Colletotrichum* Species. *Cells* **2021**, *10*, 449. [CrossRef]
21. Leonardi, G.R.; Aiello, D.; Camilleri, G.; Piattino, V.; Polizzi, G.; Guarnaccia, V. A new disease of kumquat (Fortunella margarita) caused by Colletotrichum karsti: Twig and branch dieback. *Phytopathol. Mediterr.* **2023**, *62*, 333–348. [CrossRef]
22. Ismail, M.; Zhang, J. Post-harvest Citrus Diseases and their control. *Outlooks Pest Manag.* **2004**, *15*, 29–35. [CrossRef]
23. Brown, G.E.; Eckert, J.W. Diplodia stem-end rot. *Compend. Citrus Dis.* **2000**, *2*, 43–44.
24. Zhang, J. Lasiodiplodia theobromae in Citrus Fruit (Diplodia Stem-End Rot). In *Postharvest Decay: Control Strategies*; Academic Press: Cambridge, MA, USA, 2014; pp. 309–335.
25. Lim, L.; Mohd, M.H.; Zakaria, L. Identification and pathogenicity of *Diaporthe* species associated with stem-end rot of mango (*Mangifera indica* L.). *Eur. J. Plant Pathol.* **2019**, *155*, 687–696. [CrossRef]
26. Guimarães, J.E.R.; de la Fuente, B.; Pérez-Gago, M.B.; Andradas, C.; Carbó, R.; Mattiuz, B.H.; Palou, L. Antifungal activity of GRAS salts against Lasiodiplodia theobromae in vitro and as ingredients of hydroxypropyl methylcellulose-lipid composite edible coatings to control Diplodia stem-end rot and maintain postharvest quality of citrus fruit. *Int. J. Food Microbiol.* **2019**, *301*, 9–18. [CrossRef] [PubMed]
27. Awan, Q.N.; Akgül, D.S.; Unal, G. First Report of *Lasiodiplodia pseudotheobromae* Causing Postharvest Fruit Rot of Lemon in Turkey. *Plant Dis.* **2016**, *100*, 2327. [CrossRef]
28. Huang, F.; Hou, X.; Dewdney, M.M.; Fu, Y.; Chen, G.Q.; Hyde, K.D.; Li, H.Y. Diaporthe species occurring on citrus in China. *Fungal Divers.* **2013**, *61*, 237–250. [CrossRef]
29. Kucharek, T.; Whiteside, J.O.; Brown, E. Melanose and Phomopsis Stem-End Rot of Citrus. In *Plant Pathology Fact Sheet*; Florida Cooperative Extension Service; Institute of Food and Agricultural Sciences, University of Florida: Gainesville, FL, USA, 2000; pp. 26–30.
30. Phillips, A.J.L.; Alves, A.; Abdollahzadeh, J.; Slippers, B.; Wingfield, M.J.; Groenewald, J.Z.; Crous, P.W. The Botryosphaeriaceae: Genera and species known from culture. *Stud. Mycol.* **2013**, *76*, 51–167. [CrossRef]
31. Slippers, B.; Boissin, E.; Phillips, A.J.L.; Groenewald, J.Z.; Lombard, L.; Wingfield, M.J.; Postma, A.; Burgess, T.; Crous, P.W. Phylogenetic lineages in the *Botryosphaeriales*: A systematic and evolutionary framework. *Stud. Mycol.* **2013**, *76*, 31–49. [CrossRef]
32. Batista, E.; Lopes, A.; Alves, A. What do we know about Botryosphaeriaceae? An overview of a worldwide cured dataset. *Forests* **2021**, *12*, 313. [CrossRef]
33. Bautista-Cruz, M.A.; Almaguer-Vargas, G.; Leyva-Mir, S.G.; Colinas-León, M.T.; Correia, K.C.; Camacho-Tapia, M.; Robles-Yerena, L.; Michereff, S.J.; Tovar-Pedraza, J.M. Phylogeny, Distribution, and Pathogenicity of *Lasiodiplodia Species* Associated with Cankers and Dieback Symptoms of Persian Lime in Mexico. *Plant Dis.* **2019**, *103*, 1156–1165. [CrossRef]
34. El-Ganainy, S.M.; Ismail, A.M.; Iqbal, Z.; Elshewy, E.S.; Alhudaib, K.A.; Almaghasla, M.I.; Magistà, D. Diversity among *Lasiodiplodia* Species Causing Dieback, Root Rot and Leaf Spot on Fruit Trees in Egypt, and a Description of *Lasiodiplodia newvalleyensis* sp. nov. *J. Fungi* **2022**, *8*, 1203. [CrossRef]
35. Polizzi, G.; Aiello, D.; Vitale, A.; Giuffrida, F.; Groenewald, J.Z.; Crous, P.W. First Report of Shoot Blight, Canker, and Gummosis Caused by Neoscytalidium dimidiatum on Citrus in Italy. *Plant Dis.* **2009**, *93*, 1215. [CrossRef]
36. Xiao, X.E.; Wang, W.; Crous, P.W.; Wang, H.K.; Jiao, C.; Huang, F.; Pu, Z.X.; Zhu, Z.R.; Li, H.Y. Species of Botryosphaeriaceae associated with citrus branch diseases in China. *Persoonia* **2021**, *47*, 106–135. [CrossRef]
37. Sultana, R.; Islam, M.S.; Rahman, H.; Alam, M.S.; Islam, M.A.; Sikdar, B. Characterization of Lasiodiplodia pseudotheobromae associated with citrus stem-end rot disease in Bangladesh. *Int. J. Biosci.* **2018**, *13*, 252–262.
38. Guarnaccia, V.; Groenewald, J.Z.; Woodhall, J.; Armengol, J.; Cinelli, T.; Eichmeier, A.; Ezra, D.; Fontaine, F.; Gramaje, D.; Gutierrez-Aguirregabiria, A.; et al. diversity and pathogenicity revealed from a broad survey of grapevine diseases in Europe. *Persoonia* **2018**, *40*, 135–153. [CrossRef] [PubMed]
39. Gomes, R.R.; Glienke, C.; Videira, S.I.; Lombard, L.; Groenewald, J.Z.; Crous, P.W. Diaporthe: A genus of endophytic, saprobic and plant pathogenic fungi. *Persoonia* **2013**, *31*, 1–41. [CrossRef] [PubMed]

40. Aiello, D.; Guarnaccia, V.; Costanzo, M.B.; Leonardi, G.R.; Epifani, F.; Perrone, G.; Polizzi, G. Woody Canker and Shoot Blight Caused by Botryosphaeriaceae and Diaporthaceae on Mango and Litchi in Italy. *Horticulturae* **2022**, *8*, 330. [CrossRef]
41. Guarnaccia, V.; Vitale, A.; Cirvilleri, G.; Aiello, D.; Susca, A.; Epifani, F.; Perrone, G.; Polizzi, G. Characterisation and pathogenicity of fungal species associated with branch cankers and stem-end rot of avocado in Italy. *Eur. J. Plant Pathol.* **2016**, *146*, 963–976. [CrossRef]
42. Hilario, S.; Santos, L.; Alves, A. Diversity and Pathogenicity of *Diaporthe* Species Revealed from a Survey of Blueberry Orchards in Portugal. *Agriculture* **2021**, *11*, 1271. [CrossRef]
43. Lombard, L.; van Leeuwen, G.C.M.; Guarnaccia, V.; Polizzi, G.; van Rijswick, P.C.J.; Rosendahl, K.; Gabler, J.; Crous, P.W. *Diaporthe* species associated with *Vaccinium*, with specific reference to Europe. *Phytopathol. Mediterr.* **2014**, *53*, 287–299.
44. Manawasinghe, I.S.; Dissanayake, A.J.; Li, X.H.; Liu, M.; Wanasinghe, D.N.; Xu, J.P.; Zhao, W.S.; Zhang, W.; Zhou, Y.Y.; Hyde, K.D.; et al. High Genetic Diversity and Species Complexity of *Diaporthe* Associated with Grapevine Dieback in China. *Front. Microbiol.* **2019**, *10*, 473533. [CrossRef] [PubMed]
45. Martino, I.; Tabone, G.; Giordano, R.; Gullino, M.L.; Guarnaccia, V. First Report of *Diaporthe eres* Causing Stem Blight and Dieback on Highbush Blueberry (*Vaccinium corymbosum*) in Italy. *Plant Dis.* **2023**, *107*, 1236. [CrossRef] [PubMed]
46. Udayanga, D.; Castlebury, L.A.; Rossman, A.Y.; Chukeatirote, E.; Hyde, K.D. The *Diaporthe sojae* species complex: Phylogenetic re-assessment of pathogens associated with soybean, cucurbits and other field crops. *Fungal Biol.* **2015**, *119*, 383–407. [CrossRef]
47. Udayanga, D.; Castlebury, L.A.; Rossman, A.Y.; Hyde, K.D. Species limits in *Diaporthe*: Molecular re-assessment of *D-citri*, *D-cytosporella*, *D-foeniculina* and *D-rudis*. *Persoonia* **2014**, *32*, 83–101. [CrossRef]
48. Chaisiri, C.; Liu, X.Y.; Lin, Y.; Li, J.B.; Xiong, B.; Luo, C.X. Phylogenetic Analysis and Development of Molecular Tool for Detection of *Diaporthe citri* Causing Melanose Disease of Citrus. *Plants* **2020**, *9*, 329. [CrossRef] [PubMed]
49. Mondal, S.N.; Vicent, A.; Reis, R.F.; Timmer, L.W. Saprophytic colonization of citrus twigs by Diaporthe citri and factors affecting pycnidial production and conidial survival. *Plant Dis.* **2007**, *91*, 387–392. [CrossRef]
50. Chen, G.Q.; Jiang, L.Y.; Xu, F.S.; Xu, F.; Li, H.Y. In vitro and in vivo screening of fungicides for controlling citrus melanose caused by Diaporthe citri. *J. Zhejiang Univ. Agric. Life Sci.* **2010**, *36*, 440–444.
51. Guarnaccia, V.; Crous, P.W. Species of *Diaporthe* on *Camellia* and *Citrus* in the Azores Islands. *Phytopathol. Mediterr.* **2018**, *57*, 307–319. [CrossRef]
52. Jiang, L.; Xu, F.; Huang, Z.; Huang, F.; Chen, G.; Li, H. Occurrence and control of citrus melanose caused by Diaporthe citri. *Acta Agric. Zhejiangensis* **2012**, *24*, 647–653.
53. White, T.J.; Bruns, T.; Lee, S.; Taylor, J. Amplification and direct sequencing of fungal ribosomal RNA genes for phylogenetics. *PCR Protoc. Guide Methods Appl.* **1990**, *18*, 315–322.
54. Carbone, I.; Kohn, L.M. A method for designing primer sets for speciation studies in filamentous ascomycetes. *Mycologia* **1999**, *91*, 553–556. [CrossRef]
55. Glass, N.L.; Donaldson, G.C. Development of primer sets designed for use with the PCR to amplify conserved genes from filamentous ascomycetes. *Appl. Environ. Microbiol.* **1995**, *61*, 1323–1330. [CrossRef] [PubMed]
56. O'Donnell, K.; Cigelnik, E. Two divergent intragenomic rDNA ITS2 types within a monophyletic lineage of the fungusfusariumare nonorthologous. *Mol. Phylogenet. Evol.* **1997**, *7*, 103–116. [CrossRef]
57. Pavlic, D.; Slippers, B.; Coutinho, T.A.; Wingfield, M.J. Multiple gene genealogies and phenotypic data reveal cryptic species of the Botryosphaeriaceae: A case study on the *Neofusicoccum parvum/N. ribis* complex. *Mol. Phylogenet. Evol.* **2009**, *51*, 259–268. [CrossRef]
58. Boratyn, G.M.; Camacho, C.; Cooper, P.S.; Coulouris, G.; Fong, A.; Ma, N.; Madden, T.L.; Matten, W.T.; McGinnis, S.D.; Merezhuk, Y.; et al. BLAST: A more efficient report with usability improvements. *Nucleic Acids Res.* **2013**, *41*, W29–W33. [CrossRef] [PubMed]
59. Katoh, K.; Standley, D.M. MAFFT Multiple Sequence Alignment Software Version 7: Improvements in Performance and Usability. *Mol. Biol. Evol.* **2013**, *30*, 772–780. [CrossRef]
60. Kumar, V.; Reinartz, W. Creating Enduring Customer Value. *J. Mark.* **2016**, *80*, 36–68. [CrossRef]
61. Zhang, W.; Groenewald, J.Z.; Lombard, L.; Schumacher, R.K.; Phillips, A.J.L.; Crous, P.W. Evaluating species in Botryosphaeriales. *Persoonia* **2021**, *46*, 63–115. [CrossRef] [PubMed]
62. Du, Z.; Fan, X.L.; Hyde, K.D.; Yang, Q.; Liang, Y.M.; Tian, C.M. Phylogeny and morphology reveal two new species of Diaporthe from *Betula* spp. in China. *Phytotaxa* **2016**, *269*, 90–102. [CrossRef]
63. Nylander, J. *MrModeltest v. 2 Program Distributed by the Author*; Evolutionary Biology Centre, Uppsala University: Uppsala, Sweden, 2004.
64. Ronquist, F.; Huelsenbeck, J.P. MrBayes 3: Bayesian phylogenetic inference under mixed models. *Bioinformatics* **2003**, *19*, 1572–1574. [CrossRef]
65. Cummings, M.P. PAUP* Phylogenetic Analysis Using Parsimony (* and Other Methods). In *Dictionary of Bioinformatics Computational Biology*; John Wiley & Sons Inc.: Hoboken, NJ, USA, 2004.
66. Page, R.D.M. Tree View: An application to display phylogenetic trees on personal computers. *Bioinformatics* **1996**, *12*, 357–358. [CrossRef]
67. Smith, H.; Wingfield, M.J.; Crous, P.W.; Coutinho, T.A. Sphaeropsis sapinea and Botryosphaeria dothidea endophytic in Pinus spp and Eucalyptus spp in South Africa. *S. Afr. J. Bot.* **1996**, *62*, 86–88. [CrossRef]
68. Rayner, R.W. *A Mycological Colour Chart*; Commonwealth Mycological Institute: Kew, Australia, 1970.

69. Hau, B.; Kranz, J. Mathematics and statistics for analyses in epidemiology. In *Epidemics of Plant Diseases: Mathematical Analysis and Modeling*; Springer: Berlin/Heidelberg, Germany, 1990; pp. 12–52.
70. López-Moral, A.; Raya-Ortega, M.C.; Agustí-Brisach, C.; Roca, L.F.; Lovera, M.; Luque, F.; Arquero, O.; Trapero, A. Morphological, pathogenic, and molecular characterization of Colletotrichum acutatum isolates causing almond anthracnose in Spain. *Plant Dis.* **2017**, *101*, 2034–2045. [CrossRef]
71. Aiello, D.; Carrieri, R.; Guarnaccia, V.; Vitale, A.; Lahoz, E.; Polizzi, G. Characterization and pathogenicity of colletotrichum gloeosporioides and C. karstii causing preharvest disease on citrus sinensis in Italy. *J. Phytopathol.* **2015**, *163*, 168–177. [CrossRef]
72. Steel, R.G.; Torrie, J.H. *Bioestadística: Principios y Procedimientos*; McGraw-Hill: New York, NY, USA, 1985.
73. Software, A. *Statistix 10 User's Manual*; Analytical Software: Tallahassee, FL, USA, 2013.
74. Karadžić, D.; Stanivuković, Z.; Milanović, S.; Sikora, K.; Radulović, Z.; Račko, V.; Kardošová, M.; Ďurkovič, J.; Milenković, I. Development of Neonectria punicea pathogenic symptoms in juvenile Fraxinus excelsior trees. *Front. Plant Sci.* **2020**, *11*, 592260. [CrossRef] [PubMed]
75. Crous, P.W.; Wingfield, M.J.; Richardson, D.M.; Le Roux, J.J.; Strasberg, D.; Edwards, J.; Roets, F.; Hubka, V.; Taylor, P.W.; Heykoop, M.; et al. Fungal Planet description sheets: 400–468. *Persoonia* **2016**, *36*, 316–458. [CrossRef] [PubMed]
76. Abdollahzadeh, J.; Javadi, A.; Mohammadi Goltapeh, E.; Zare, R.; Phillips, A.J. Phylogeny and morphology of four new species of Lasiodiplodia from Iran. *Persoonia* **2010**, *25*, 1–10. [CrossRef] [PubMed]
77. Netto, M.S.B.; Lima, W.G.; Correia, K.C.; Da Silva, C.F.B.; Thon, M.; Martins, R.B.; Miller, R.N.G.; Michereff, S.J.; Câmara, M.P.S. Analysis of phylogeny, distribution, and pathogenicity of *Botryosphaeriaceae* species associated with gummosis of *Anacardium* in Brazil, with a new species of *Lasiodiplodia*. *Fungal Biol.* **2017**, *121*, 437–451. [CrossRef] [PubMed]
78. Li GuoQing Li, G.; Arnold, R.J.; Liu FeiFei Liu, F.; Li JieQiong Li, J.; Chen ShuaiFei Chen, S. Identification and pathogenicity of Lasiodiplodia species from Eucalyptus urophylla × grandis, Polyscias balfouriana and Bougainvillea spectabilis in southern China. *J. Phytopathol.* **2015**, *163*, 956–967.
79. Negi, N.; Krishna, R.; Meena, R.K.; Pandey, A.; Bhandari, M.S.; Pandey, S. First report of *Lasiodiplodia iraniensis* causing leaf spot disease of *Eucalyptus* in India. *Physiol. Mol. Plant Pathol.* **2023**, *127*, 102113. [CrossRef]
80. Al-Sadi, A.M.; Al-Wehaibi, A.N.; Al-Shariqi, R.M.; Al-Hammadi, M.S.; Al-Hosni, I.A.; Al-Mahmooli, I.H.; Al-Ghaithi, A.G. Population Genetic Analysis Reveals Diversity in Lasiodiplodia Species Infecting Date Palm, Citrus, and Mango in Oman and the UAE. *Plant Dis.* **2013**, *97*, 1363–1369. [CrossRef] [PubMed]
81. Marques, M.W.; Lima, N.B.; de Morais, M.A.; Barbosa, M.A.G.; Souza, B.O.; Michereff, S.J.; Phillips, A.J.L.; Câmara, M.P.S. Species of *Lasiodiplodia* associated with mango in Brazil. *Fungal Divers.* **2013**, *61*, 181–193. [CrossRef]
82. Fayyaz, A.; Bonello, P.; Tufail, M.R.; Amrao, L.; Habib, A.; Gai, Y.; Sahi, S.T. First report of citrus withertip (tip dieback), a disease complex caused by Colletotrichum siamense and Lasiodiplodia iraniensis, on Citrus reticulata cv. Kinnow in Punjab, Pakistan. *Plant Dis.* **2018**, *102*, 2659. [CrossRef]
83. Chen, J.; Zhu, Z.; Fu, Y.; Cheng, J.; Xie, J.; Lin, Y. Identification of *Lasiodiplodia pseudotheobromae* Causing Fruit Rot of Citrus in China. *Plants* **2021**, *10*, 202. [CrossRef]
84. Thompson, S.M.; Grams, R.A.; Neate, S.M.; Shivas, R.G.; Ryley, M.J.; Tan, Y.P.; Aitken, E.A.B.; Wright, G.C.; O'Connor, D.J. First Reports of *Diaporthe kongii*, *D. masirevicii*, and *D. ueckerae* Associated with Stem and Peg Dieback on Peanut in Australia. *Plant Dis.* **2018**, *102*, 1459. [CrossRef]
85. Gao, Y.H.; Liu, F.; Cai, L. Unravelling *Diaporthe* species associated with *Camellia*. *Syst. Biodivers.* **2016**, *14*, 102–117. [CrossRef]
86. Liao, W.J.; Luo, L.F.; Zou, D.X.; Wu, Y.J.; Chen, S.Y.; Luo, J. First Report of Branch Blight Caused by *Diaporthe ueckerae* on *Eucalyptus citriodora* in China. *Plant Dis.* **2023**, *107*, 563. [CrossRef]
87. López-Cardona, N.; Guevara-Castro, A.; Gañán-Betancur, L.; Amaya-Gomez, C.V. First Report of Diaporthe ueckerae Causing Stem Canker on Soybean (*Glycine max*) in Colombia. *Plant Dis.* **2021**, *105*, 4162. [CrossRef]
88. Wang, Y.C.; Liu, J.H.; Huang, C.C.; Hong, C.F. First Report of Dragon Fruit (Hylocereus undatus) Stem Rot Caused by Diaporthe ueckerae in Taiwan. *Plant Dis.* **2022**, *106*, 1527. [CrossRef]
89. Serrato-Diaz, L.M.; Rivera-Vargas, L.I.; French-Monar, R.D. First Report of *Diaporthe pseudomangiferae* Causing Inflorescence Rot, Rachis Canker, and Flower Abortion of Mango. *Plant Dis.* **2014**, *98*, 1004–1005. [CrossRef]
90. Li, S.; Xu, L.; Zhang, W. First Report of Postharvest Stem-End Rot of Mango Fruit (*Mangifera indica*) Caused by *Diaporthe pseudomangiferae* in China. *Plant Dis.* **2023**, *107*, 582. [CrossRef]
91. Serrato-Diaz, L.M.; Ayala-Silva, T.; Goenaga, R. First Report of *Diaporthe tulliensis* and *D. pseudomangiferae* Causing Cacao Pod Rot in Puerto Rico. *Plant Dis.* **2022**, *106*, 2530. [CrossRef]
92. Seungeun, G.; Wonyong, K.; Kwang-Yeol, Y. Emergence of multiple Diaporthe species causing kiwifruit rot and occurrence of resistance to a methyl benzimidazole carbamate fungicide in South Korea. *Crop Prot.* **2022**, *158*, 106016. [CrossRef]
93. Yi, R.; Chen, Y.; Han, J.; Hu, Q.; Li, H.; Wu, H. Identification and biological characteristics of Diaporthe ueckerae causing dieback disease on Michelia shiluensis. *Sci. Silvae Sin.* **2018**, *54*, 80–88.
94. PRISM Climate Group. PRISM Spatial Climate Datasets for the Coterminous United States. *Oregon State University*. 2022. Available online: https://prism.oregonstate.edu/ (accessed on 1 November 2023).
95. Batista, E.; Lopes, A.; Miranda, P.; Alves, A. Can species distribution models be used for risk assessment analyses of fungal plant pathogens? A case study with three Botryosphaeriaceae species. *Eur. J. Plant Pathol.* **2023**, *165*, 41–56. [CrossRef]

96. Slippers, B.; Wingfield, M.J. Botryosphaeriaceae as endophytes and latent pathogens of woody plants: Diversity, ecology and impact. *Fungal Biol. Rev.* **2007**, *21*, 90–106. [CrossRef]
97. Li, L.; Mohd, M.; Mohamed Nor, N.; Subramaniam, S.; Latiffah, Z. Identification of Botryosphaeriaceae associated with stem-end rot of mango (*Mangifera indica* L.) in Malaysia. *J. Appl. Microbiol.* **2021**, *130*, 1273–1284. [CrossRef]
98. Sutton, T.B.; Aldwinckle, H.S.; Agnello, A.M.; Walgenbach, J.F. *Compendium of Apple and Pear Diseases and Pests*, 2nd ed.; American Phytopathological Society: St. Paul, MN, USA, 2014.
99. Aćimović, S.G.; Rooney-Latham, S.; Albu, S.; Grosman, D.M.; Doccola, J.J. Characterization and pathogenicity of Botryosphaeriaceae fungi associated with declining urban stands of coast redwood in California. *Plant Dis.* **2018**, *102*, 1950–1957. [CrossRef]
100. Schoeneweiss, D.F. Role of environmental stress in diseases of woody plants. *Plant Dis.* **1981**, *65*, 308–314. [CrossRef]
101. Wene, E.; Schoeneweiss, D. Localized freezing predisposition to Botryosphaeria canker in differentially frozen woody stems. *Can. J. Bot.* **1980**, *58*, 1455–1458. [CrossRef]
102. Ganesan, S.; Kumari, N.; Sahu, S.; Pattanaik, M.; Kishore, K. Identification of Lasiodiplodia species inciting stem rot of dragon fruit in India through polyphasic approach. *3 Biotech* **2023**, *13*, 333.
103. Mohankumar, V.; Dann, E.K.; Akinsanmi, O.A. Diversity and Pathogenicity of Botryosphaeriaceae Associated with Macadamia Branch Dieback in Australia. *Plant Dis.* **2022**, *106*, 2576–2582. [CrossRef]
104. Dutta, S.K.; Gurung, G.; Yadav, A.; Laha, R.; Mishra, V.K. Factors associated with citrus fruit abscission and management strategies developed so far: A review. *N. Z. J. Crop Hortic. Sci.* **2022**, *51*, 467–488. [CrossRef]
105. Moreira, R.R.; Machado, F.J.; Lanza, F.E.; Trombin, V.G.; Bassanezi, R.B.; De Miranda, M.P.; Barbosa, J.C.; Da Silva, G.J., Jr.; Behlau, F. Impact of diseases and pests on premature fruit drop in sweet orange orchards in Sao Paulo state citrus belt, Brazil. *Pest Manag. Sci.* **2022**, *78*, 2643–2656. [CrossRef]
106. Tang, L.; Chhajed, S.; Vashisth, T. Preharvest Fruit Drop in Huanglongbing-affected 'Valencia' Sweet Orange. *J. Am. Soc. Hortic. Sci.* **2019**, *144*, 107–117. [CrossRef]
107. Zhao, W.; Gottwald, T.; Bai, J.H.; McCollum, G.; Irey, M.; Plotto, A.; Baldwin, E. Correlation of *Diplodia* (*Lasiodiplodia theobromae*) infection, huanglongbing, ethylene production, fruit removal force and pre-harvest fruit drop. *Sci. Hortic.* **2016**, *212*, 162–170. [CrossRef]
108. Moral, J.; Morgan, D.; Trapero, A.; Michailides, T.J. Ecology and epidemiology of diseases of nut crops and olives caused by Botryosphaeriaceae fungi in California and Spain. *Plant Dis.* **2019**, *103*, 1809–1827. [CrossRef]
109. Lawrence, D.P.; Travadon, R.; Baumgartner, K. Diversity of Diaporthe species associated with wood cankers of fruit and nut crops in northern California. *Mycologia* **2015**, *107*, 926–940. [CrossRef]